

Chapter 2

Latent Olefin Metathesis Catalysts Featuring Chelating Alkylidenes

This chapter was taken in part from:

Ung, T.; Hejl, A.; Grubbs, R. H.; Schrodi, Y. *Organometallics* **2004**, 23, 5399–5401.

Hejl, A.; Day, M. W.; Grubbs, R. H. *Organometallics* **2006**, 25, 6149–6154.

Latent Olefin Metathesis Catalysts Featuring Chelating Alkylidenes

Introduction

The development of well-defined transition metal complexes capable of catalyzing olefin metathesis has been particularly important in expanding the utility of this reaction.¹ In search of high activity and fast initiation in a range of metathesis reactions, the incorporation of *N*-heterocyclic carbene (NHC) ligands, such as H₂IMes (H₂IMes = 1,3-dimesityl-imidazolidine-2-ylidene), has led to versatile catalysts **2.1–2.3** (Chart 2.1).² For some processes it is desirable that catalyst initiation be controllable. Much less work has focused on decreasing the initiation rate of ruthenium-based catalysts. In these cases, the use of a trigger such as photoirradiation, addition of acid, or heating the sample can help to control initiation. Efficient ring-opening metathesis polymerization (ROMP) reactions require adequate mixing of monomer and catalyst before polymerization occurs. For these applications, catalysts that initiate polymerization at a high rate only upon heating would be desirable. However, both **2.1**³ and **2.2**⁴ are competent metathesis catalysts at or below room temperature, so alone are not well suited for applications where catalyst latency is beneficial.

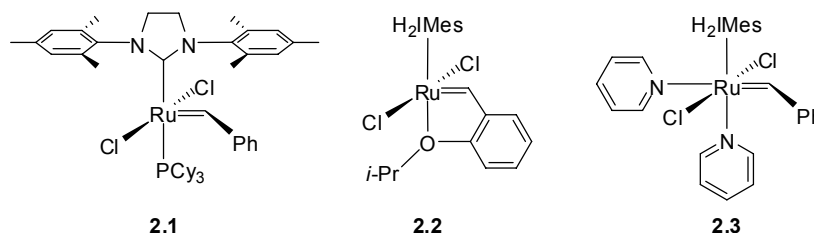


Chart 2.1. Commonly Used Ruthenium Olefin Metathesis Catalysts

Experimental studies have shown that, for the majority of ruthenium catalysts, dissociation of a donor ligand provides entry to the catalytic cycle.⁵ Several design strategies for slowing ligand dissociation can be envisioned. An important consideration is that the method used to slow initiation should not disrupt the catalyst activity. The addition of excess phosphine to the reaction can serve to slow initiation as shown in case I (Figure 2.1).⁶ Unfortunately the addition of phosphine commonly results in propagation rates also being reduced.

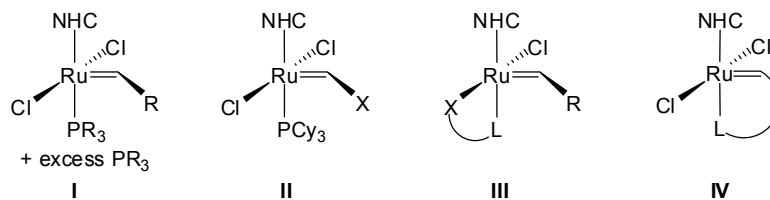


Figure 2.1. Strategies to control catalyst initiation.

Another strategy to slow catalyst initiation is to replace the Schrock-type ruthenium carbene with a Fischer carbene (Type II, Figure 2.1). This approach has been used to generate several latent metathesis catalysts with Fischer carbenes featuring oxygen, sulfur, and nitrogen substitution (Chart 2.2).^{7,8} In some cases, the decrease in activity with these systems is so great that they are considered metathesis-inactive. In fact, addition of ethyl vinyl ether to form a Fischer carbene complex is a standard method of quenching ROMP reactions.⁹

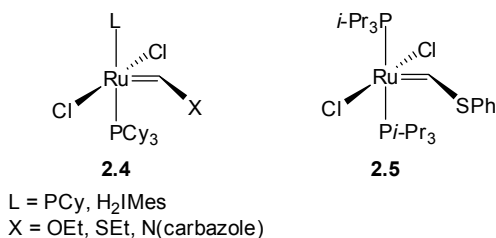


Chart 2.2. Olefin Metathesis Catalysts with Fischer Carbene Ligands

The chelate effect can be exploited by using bidentate systems to tether a neutral, dissociating ligand, L, to the catalyst (Type III, Figure 2.1). The presence of a chelate allows the use of donors, such as pyridine, known to bind weakly to ruthenium catalysts. Several examples with bidentate ligands have appeared in the literature. Salicylaldimine-based systems have been synthesized by Grubbs (**2.6**)¹⁰ and Verpoort (**2.7**)¹¹ and were found to show activity only at elevated temperatures (Chart 2.3). Herrmann has tested catalysts with pyridine–alkoxide ligands (**2.8**) that showed enhanced activity in ROMP when heated, an effect attributed to increased dissociation of the pyridine portion at elevated temperatures.¹² Tethering the donor through the anionic portion has the disadvantage that the dissociating portion is always held in close proximity to the metal center. While this helps to control the initiation it can also prevent efficient

propagation. Furthermore, it has been observed that replacing the halide ligands with oxygen donors such as those found in **2.6–2.8** can reduce catalyst activity.¹³

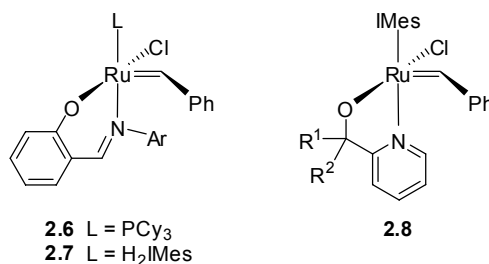
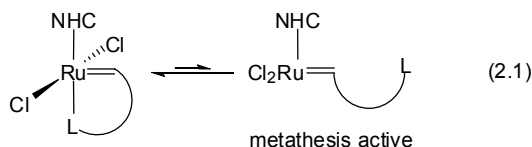


Chart 2.3. Olefin Metathesis Catalysts with Bidentate L–X Type Ligands

An alternative approach to exploit the chelate effect is to tether the dissociating ligand to the ruthenium center via the alkylidene group. If the donor ligand, L, is attached to the alkylidene, chelation favors the precatalyst over the metathesis active form (eq 2.1). After a catalytic turnover, however, the donor will no longer be tethered to the metal center and catalysis should proceed quickly. This switch in catalyst structure from chelated to nonchelated once catalysis begins makes this a more attractive method for designing thermally latent catalysts than the other strategies.



Several examples of catalysts featuring the chelating alkylidene motif have been synthesized (Chart 2.4). The most commonly used chelating framework is the isopropyl ether system **2.2** developed by Hoveyda. While **2.2** features a chelating oxygen donor, this catalyst is active below room temperature suggesting that the ether is not strong enough to render **2.2** latent.¹⁴ Grela has added electron-donating groups to this system to provide thermally switchable catalysts.¹⁵ Fürstner¹⁶ and, more recently, Slugovc¹⁷ have reported catalysts featuring ester- or aldehyde-substituted benzylidenes (**2.9**) that show reduced activity at room temperature. van der Schaaf and coworkers have employed the 2-(3-butenyl)pyridine ligand with phosphine-based catalysts to synthesize latent pyridine-containing systems (**2.10**).

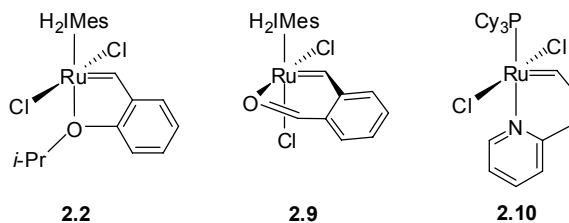


Chart 2.4. Olefin Metathesis Catalysts Featuring Chelating Alkylidenes

This project was designed to develop new latent, ruthenium-based olefin metathesis catalysts. An NHC ligand would provide highly active systems, and tethering the dissociating donor ligand through the alkylidene would control the activity. The dissociating portion could be varied to explore the coordination of several different types of donors. Ideally, stable catalysts with an easily tunable range of initiation behaviors would be prepared.

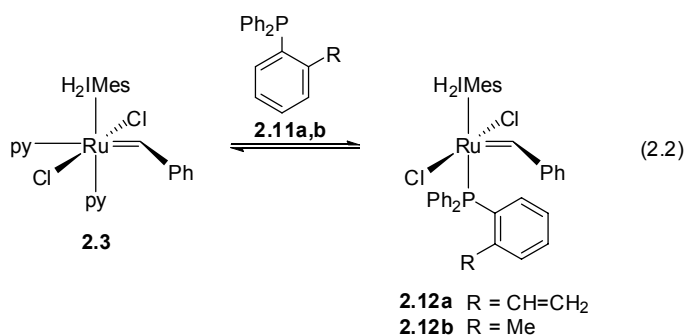
Results and Discussion

Chelating Phosphines

The first approach attempted was to prepare chelating phosphine ligands. Catalyst **2.1** was based on a dissociating phosphine ligand and it was expected that tethering the phosphine portion should result in a catalyst demonstrating latent behavior. Additionally, the phosphorous substituents could be altered to change the steric and electronic properties of the ligand. A logical choice was to begin with a ligand analogous to the ether ligand in **2.2** but replace the ether portion with a phosphine donor.

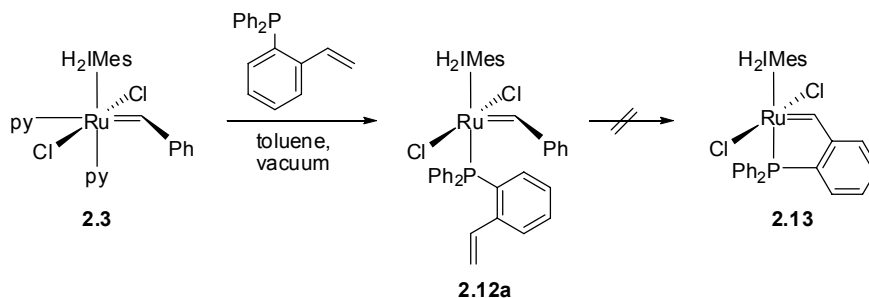
The phosphine ligand 2-(diphenylphosphino)styrene (**2.11a**) was synthesized according to known procedures.¹⁸ Pyridine-containing catalyst **2.3** was chosen as a ruthenium precursor because of its demonstrated ability to readily displace the pyridine ligands giving NHC–phosphine complexes.¹⁹ Surprisingly, reaction of **2.3** with the phosphine ligand **2.11a** did not cleanly give the phosphine-substituted complex **2.12a**. Instead, an equilibrium was established between the starting material and the desired product (eq 2.2). The presence of both ruthenium compounds was evident from the ¹H NMR spectrum, which showed resonances corresponding to both benzylidenes (19.15 ppm for **2.3** and 19.05 ppm for **2.12a**). Additionally the ³¹P NMR spectrum

showed excess amounts of phosphine **2.11a** (-4.5 ppm) as well as the desired complex (42.3 ppm).



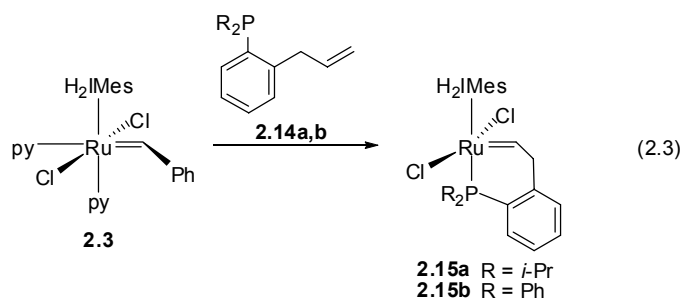
Since PPh₃ quickly displaces pyridine from **2.3**, it was suspected that the decreased binding of the phosphine ligand was a result of steric interference from the aryl ring's ortho substituent. When an excess amount of diphenyl(*o*-tolyl)phosphine was added to **2.3**, a similar equilibrium was established.

One method explored to drive the reaction to completion was to remove pyridine from the system. By performing the reaction in toluene, pyridine could be removed azeotropically on evaporation. This procedure effectively removed all pyridine from the system and gave exclusively the phosphine-bound complex **2.12a** (Scheme 2.1). Upon heating, no formation of the desired chelating phosphine complex **2.13** was observed. The inability to synthesize **2.13** may be due to several factors. Styrenes are not especially reactive substrates for olefin metathesis reactions; the presence of a large ortho-substituent decreases the reactivity even further.²⁰



Scheme 2.1. Removal of Pyridine Drives Phosphine Coordination

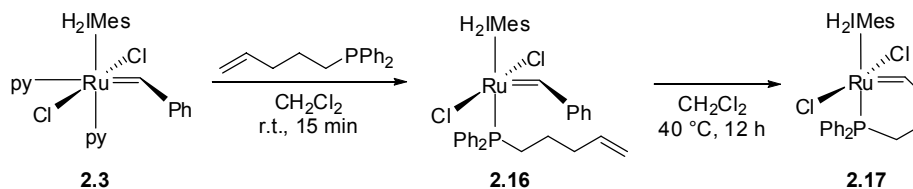
Since the rigid styrene framework prevented effective chelation, a more flexible ligand framework was targeted. Extension of the linker by one carbon by employing an allylbenzene framework was a logical approach. Phosphine ligands with an allylbenzene portion and either isopropyl or phenyl substituents were prepared (**2.14**). Reactions of these ligands with ruthenium complex **2.3** gave the desired chelated complexes (**2.15a,b**, eq 2.3). The isopropyl-substituted phosphine **2.14a** proceeded directly to give the chelated phosphine complex **2.15a**. The triaryl phosphine **2.14b** was unable to directly displace pyridine but did undergo a metathesis reaction with the allylbenzene portion to produce styrene. Subsequent azeotropic removal of pyridine allowed for the isolation of the desired chelated complex **2.15b**.



Complexes **2.15** were air- and moisture-stable, which allowed for their handling on the benchtop and purification by column chromatography in good yield. The ^1H NMR spectra were consistent with the chelated structures. In both complexes the diagnostic alkylidene protons were shifted upfield of the starting material (18.27 ppm for **2.15a** and 17.99 ppm for **2.15b**). These resonances appeared as pseudo quartets due to coupling to both the adjacent methylene protons and the coordinated ^{31}P nucleus. The ^{31}P NMR spectra showed resonances for the chelated phosphines shifted downfield of similar coordinated, non-chelating phosphine ligands (61.85 ppm for **2.15a** and 37.80 ppm for **2.15b**).

To avoid the steric interactions that hindered phosphine substitution reactions with triaryl phosphines a ligand with an alkyl tether was prepared. Upon addition of diphenyl(4-pentenyl)phosphine to **2.3**, the pyridine ligands were instantaneously and completely displaced giving **2.16** (Scheme 2.2). Successful ligand exchange was evidenced by a color change from dark green to the characteristic red color of NHC–phosphine complexes. The ^1H NMR spectrum showed a slight shift in the benzylidene proton (δ 19.05 ppm) and a ^{31}P NMR resonance at 31.7

ppm, similar to other NHC–phosphine complexes. Upon heating overnight the alkene tether underwent a metathesis reaction to “clip on” to the catalyst giving the chelated complex. Again, the resulting complex was air-stable and could be purified on the benchtop to give product **2.17** in good yield.



Scheme 2.2. Catalyst Synthesis With Alkyl-Tethered Phosphine

The NMR spectra of **2.17** supports the structure depicted in Scheme 2.2. In the ^1H NMR spectrum the alkylidene protons are shifted upfield to 18.60 ppm and appear as a clear triplet of doublets due to coupling to both the adjacent methylene protons and the phosphorus. In the ^{13}C NMR spectrum the alkylidene carbon appears at 327.24 ppm, shifted well downfield of the benzylidene precursors (~ 300 ppm).

The newly synthesized chelated phosphine catalysts were tested in the ring-closing metathesis (RCM) of diethyl diallylmalonate (**2.18**) (eq 2.4) and the results are shown in Figure 2.2. For testing latent catalysts, elevated temperatures and catalyst loadings were required, so standard conditions of 2.5 mol% catalyst in C_6D_6 were chosen and the temperature was varied. The catalytic activity was found to be quite dependent on both the linker and the phosphorus substituents. Catalyst **2.17** containing the alkyl linker, performed the slowest, likely a result of the low steric demand of the alkyl linker. The catalysts with the allylbenzene framework both catalyzed the reaction more quickly than **2.17**. Somewhat surprisingly, **2.15b** allowed the reaction to reach completion quickly at elevated temperature. These results suggest that after catalyst initiation, rebinding of the sterically encumbered phosphine is disfavored and as a result catalysis occurs more quickly. Unfortunately, full conversion was not obtained for **2.15a** and **2.17** at elevated temperatures even though uninitiated precatalyst still remained.

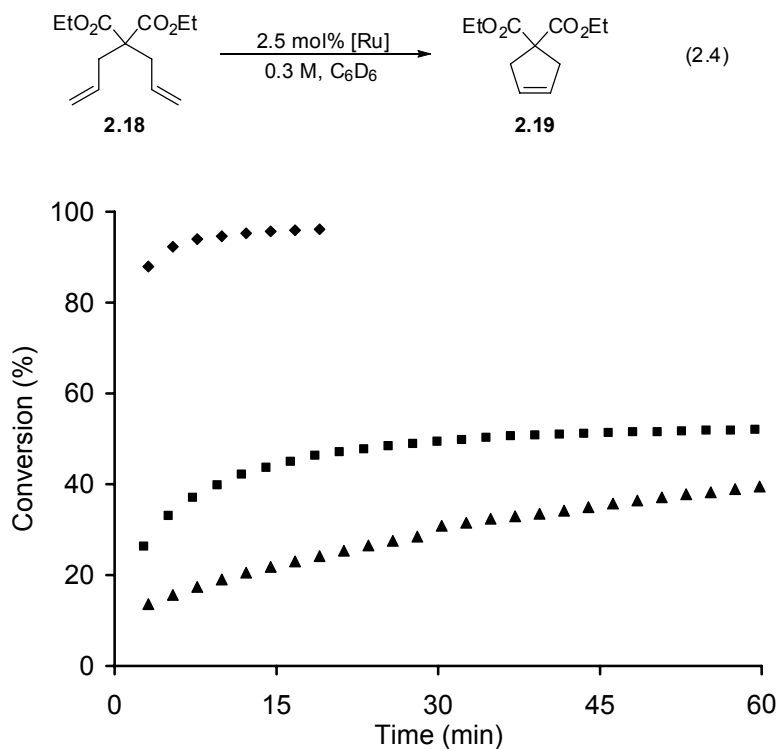


Figure 2.2. Conversion plot for RCM of **2.18** with (■) **2.15a**, (◆) **2.15b**, (▲) **2.17** (2.5 mol%, 60 °C, 0.3 M C₆D₆).

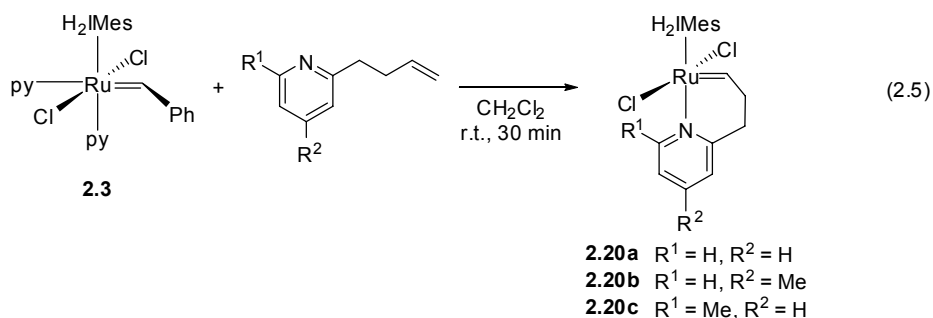
From these studies it was clear that tethering a phosphine ligand through the alkylidene produced a latent catalyst. However, rebinding of the phosphine ligand after the onset of catalysis resulted in decreased overall efficiency. Of the new catalysts prepared, **2.15b** alone catalyzed the RCM of **2.18** to completion, likely because the sterically bulky phosphine ligand could only form a weak bond to ruthenium. The air-sensitive ligand syntheses and limited range of control are additional drawbacks to the use of chelating phosphine ligands.

Pyridine Chelates

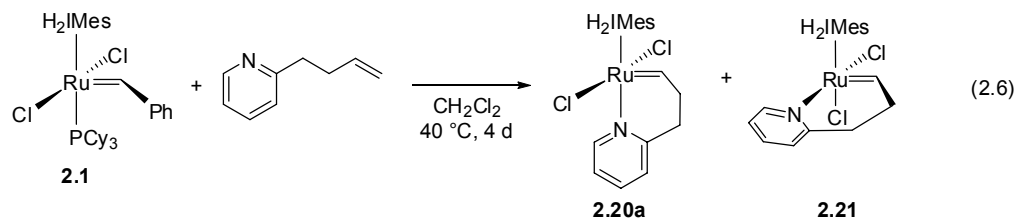
The phosphine-based chelates did provide latent catalysts but required very high temperatures and upon initiation released phosphines that inhibited the reaction. Systems that would not experience this inhibition and were active at only slightly elevated temperatures were still sought. Pyridine ligands appeared to be a good choice to satisfy these properties. In nonchelated systems such as **2.3**, pyridine was known to dissociate readily without impeding reaction progress. Chelated pyridines had been developed for use with first-generation

phosphine-based systems (as in **2.10**) and did provide slow initiating catalysts. The combination of chelating pyridine ligands and *N*-heterocyclic carbene systems seemed a promising route to high activity latent catalysts.

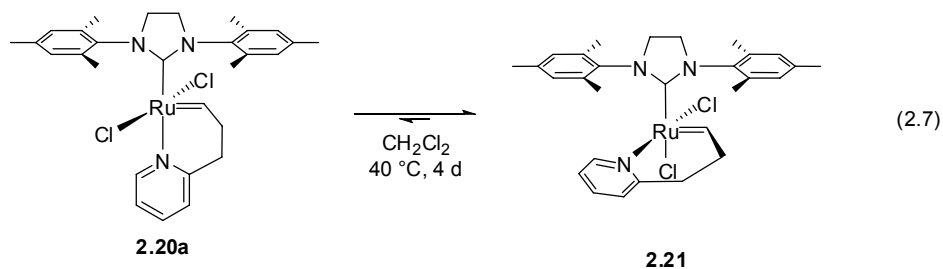
Catalyst **2.3** was reacted with 2-(3-butenyl)pyridine at room temperature to give the chelated catalyst **2.20a** in good yield (eq 2.5). This synthesis could be extended to systems with varied substitution on the pyridine ring to give catalysts with 4- or 6-methyl-substituted pyridines. The resulting catalysts were again relatively air-stable materials that could be easily handled on the benchtop. The ^1H NMR spectra of **2.20a–c** were consistent with compounds of C_s symmetry. The alkylidene protons near 18.4 ppm appeared as triplets coupled to the adjacent methylene protons. The two *para*-methyl and four *ortho*-methyl groups on the mesityl ring as well as the backbone protons on the NHC ligand appeared as singlets, showing the complexes had high symmetry.



During the synthesis of **2.20a** from **2.1**, which involved heating overnight, the slow formation of a secondary product was observed (eq 2.6). Upon heating for several days two complexes, **2.20a** and **2.21**, were obtained in a ~ 3:7 mixture. **2.21** could be isolated in pure form (albeit in reduced yield) based on its differing solubility properties. The ^1H NMR spectrum of this complex was consistent with a Ru carbene displaying C_1 symmetry. In particular, the spectrum shows six distinct methyl resonances from the mesityl rings, and four inequivalent protons on the NHC backbone and four unique protons on the alkyl tether.



When either **2.20a** or **2.21** alone is heated to 40 °C in CH₂Cl₂ over a period of several days, both formed a ~1:4 (**2.20a**:**2.21**) mixture of the two complexes (eq 2.7). This indicated that the two species are in equilibrium with a $K_{\text{eq}} = 0.28$. This equilibrium appeared to be highly solvent dependent; when **2.20a** was heated in benzene over a period of several days, no appreciable formation of **2.21** was observed. Subsequent calculations showed that the solution energies of the two isomers are very similar and supported a similar equilibrium.²¹ The solvent effects could be attributed to the large difference in dipole moment between **2.20a** and **2.21** that increased the solvation energy based on greater polarity.



Crystals suitable for X-ray analysis were obtained for **2.20a** and **2.21** and the resulting structures are shown in Figure 2.3 and Figure 2.4, respectively. Both complexes display the typical square pyramidal geometries for Ru metathesis catalysts with the alkylidene occupying the axial position. **2.20a** shows the pyridine to be trans to the NHC, (C(1)–Ru–N(3) = 170.21(4)°) and the chloride ligands also occupy trans positions (Cl(1)–Ru–Cl(2) = 164.41(1)°). This arrangement is typical for metathesis catalysts and is consistent with the C_s solution symmetry. In contrast, **2.21** shows a “side-bound” geometry with the NHC and pyridine ligands (C(1)–Ru–N(3) = 98.04(8)°) and chloride ligands (Cl(1)–Ru–Cl(2) = 85.93(2)°) oriented cis to one another, maintaining the C_1 symmetry deduced from the spectroscopic data. This cis-chloride ligand arrangement is relatively rare for ruthenium carbene complexes, but has been observed in a

handful of cases.²² The Ru–N(3) distance of 2.1355(9) Å in **2.20a** is somewhat longer than that of 2.098(2) Å in **2.21**, due to the trans influence of the NHC ligand. Similarly, the Ru–Cl(2) distance in **2.21** (2.3883(6) Å) is longer than that in **2.20a** (2.3662(3) Å).

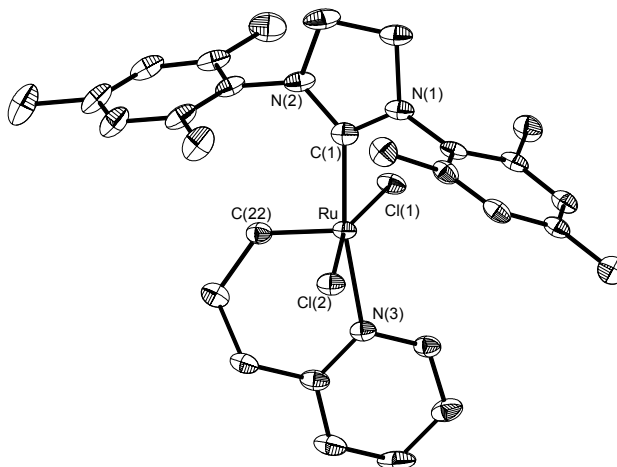


Figure 2.3. Solid-state structure of **2.20a** with thermal ellipsoids drawn at 50% probability. Selected bond distances (Å) and angles (deg): Ru–C(1) = 2.0459(10), Ru–C(22) = 1.8185(11), Ru–N(3) = 2.1355(9), Ru–Cl(1) = 2.3973(3), Ru–Cl(2) = 2.3662(3); Cl(1)–Ru–Cl(2) = 164.406(11), C(1)–Ru–N(3) = 170.21(4), C(22)–Ru–N(3) = 88.32(4).

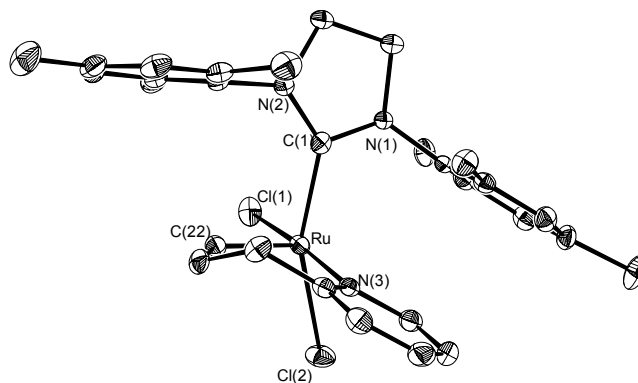


Figure 2.4. Solid-state structure of **2.21** with thermal ellipsoids drawn at 50% probability. Selected bond distances (Å) and angles (deg): Ru–C(1) = 2.024(2), Ru–C(22) = 1.811(2), Ru–N(3) = 2.0977(19), Ru–Cl(1) = 2.4000(6), Ru–Cl(2) = 2.3883(6); Cl(1)–Ru–Cl(2) = 85.93(2), C(1)–Ru–N(3) = 98.04(8), C(22)–Ru–N(3) = 92.35(10), C(1)–Ru–Cl(1) = 88.62(6), C(1)–Ru–Cl(2) = 153.74(6).

To probe the latency of the new pyridine chelates they were tested in the RCM of **2.18** at room temperature (Figure 2.5). In RCM, **2.20a** is much slower than **2.1** (< 20% conversion after 100 min for **2.20a** vs ~100% conversion for **2.1**) and **2.21** (< 2% conversion after 100 min) is much slower than **2.20a**. The difference in reactivity between **2.20a** and **2.21** can be attributed to

the fact that the pyridine ligand in **2.20a** is trans to the strongly σ -donating NHC ligand and therefore dissociates to give the active species much more quickly than in **2.21**.

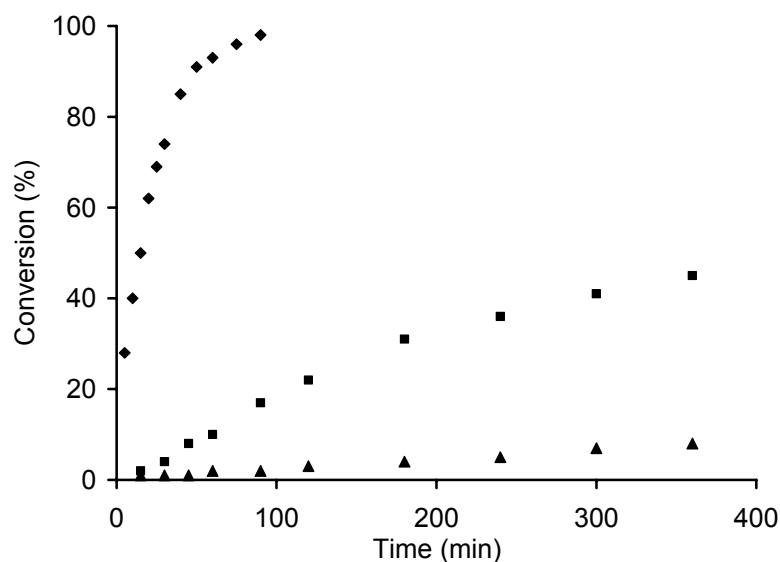


Figure 2.5. Conversion plot for RCM of **2.18** with **2.1** (◆), **2.20a** (■), and **2.21** (▲) (1.0 mol%, 25 °C, 0.1 M CH₂Cl₂).

To evaluate catalyst behavior in polymerization reactions, these complexes were tested in the ROMP of dicyclopentadiene (DCPD) (eq 2.8). In these experiments, the catalyst is added to a sample of DCPD held in a constant-temperature oil bath monitored with a thermocouple. As the strained norbornene-like double bond is opened, energy is released that heats the system, eventually resulting in a sharp rise in temperature. The resulting plots contain information about two factors: initiation rate (time to exotherm) and activity (peak temperature). This reaction is particularly useful for latent systems, because for active catalysts, such as **2.1** and **2.2**, the reaction occurs very quickly, leading to microencapsulation of the catalyst and incomplete polymerization. Figure 2.6 shows an exotherm graph of DCPD ROMP started at 30 °C for catalysts **2.20a** and **2.21**. ROMP of DCPD with **2.20a** reaches its exotherm within 3 min, while the same polymerization catalyzed by **2.21** requires more than 25 min, again highlighting a major difference between the two systems.

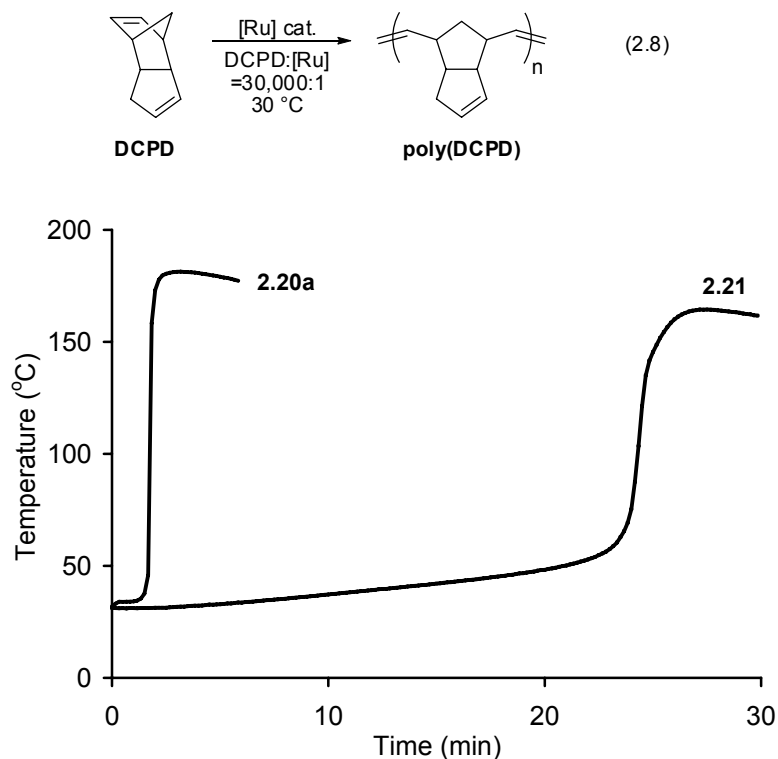


Figure 2.6. Exotherm plot for ROMP of DCPD with **2.20a**, **2.21** (30,000:1 M/C, 30 °C).

Substitution on the pyridine ring has a much less dramatic effect on catalytic activity. **2.20a** and **2.20b** show similar reactivity in the RCM of **2.18** performed at 40 °C, but **2.20c** proved to initiate faster than the others, presumably due to steric crowding of the *ortho*-methyl group (Figure 2.7). In the ROMP of DCPD, a reaction less sensitive to small reactivity differences, the three complexes **2.20a–c** were found to have very similar catalytic properties (see Experimental Section).

Grela and coworkers have recently reported metathesis catalysts based on a chelating quinoline framework similar to the pyridines used here (Chart 2.5).²³ They have also found a very similar isomerization process to convert the bottom-bound form (**2.22**) to the side-bound form (**2.23**). As in the pyridine case, the side-bound catalyst shows much lower activity than the bottom-bound species.

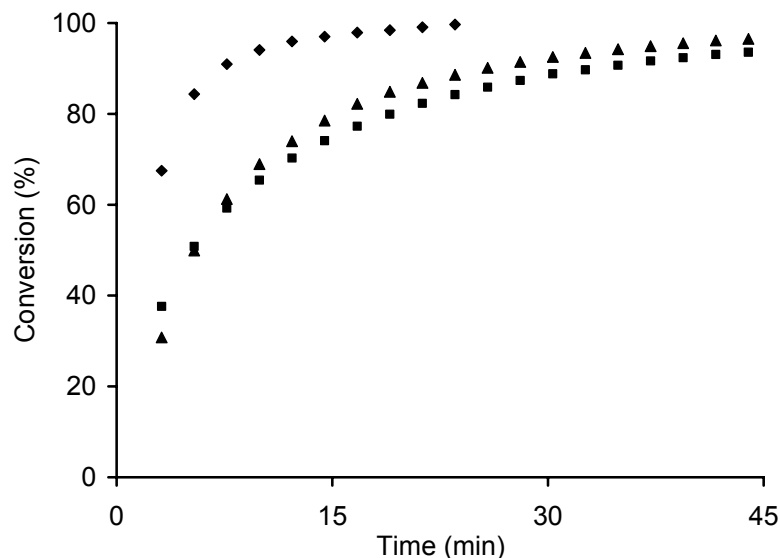


Figure 2.7. Conversion plot for RCM of **2.18** with **2.20a** (■), **2.20b** (▲), and **2.20c** (◆) (2.5 mol%, 40 °C, 0.3 M C₆D₆).

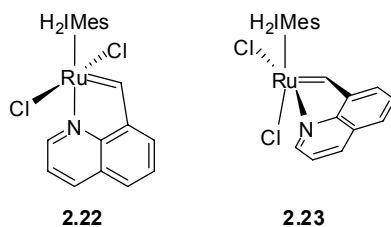


Chart 2.5. Olefin Metathesis Catalysts With Chelated Quinoline Ligand

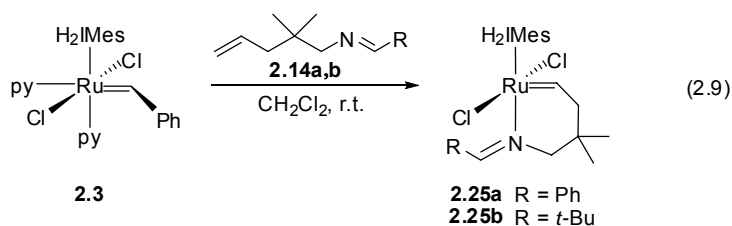
The pyridine chelates gave catalysts with significantly different metathesis activity than the phosphine systems. Varying the substitution on the pyridine ring had only a modest effect on activity, but the relative binding orientation of the pyridine ligand (side-bound vs bottom-bound) dramatically changed the catalytic activity. The difference in activity is believed to be purely due to a disparity in initiation rates, and does not reflect on the binding of olefin to an unsaturated species or on the conformation of metallacyclobutane intermediates. We cannot ignore, however, that the two binding modes are quite close in energy.

Imine Catalysts

The pyridine-derived catalysts offered desirable initiation properties, efficient catalysis and thermal switching. However, attempts to modify the initiation behavior by varying the steric

and electronic properties of the pyridine met with limited success. Catalysts such as **2.6**, based on salicyladimines showed that imines were also competent ligands for ruthenium metathesis catalysts. Moving to a chelating imine framework offered great potential to maintain latent behavior but increase the tunability by varying the steric and electronic properties of the imine donor.

The imine ligands **2.24a,b** were prepared by simple condensation of 2,2-dimethyl-4-pentenylamine with various aldehydes. The resulting unsaturated imines could then be reacted with **2.3** at room temperature to afford the imine-bound catalysts **2.25a,b** in good yields (eq 2.9). The resulting imine-bound catalysts **2.25a,b** were isolated by simple precipitation on the benchtop. The complexes could be purified by column chromatography with minimal decomposition during this process.



The ^1H NMR spectra for **2.25a,b** are consistent with the symmetric C_s structure shown in eq 2.9. The alkylidene proton resonance is especially diagnostic, appearing between 18.5 and 18.7 ppm as a triplet coupled to the adjacent methylene protons. The ^{13}C NMR spectrum shows the alkylidene carbon shifted very far downfield (~341–343 ppm), while the NHC carbon appears near 218 ppm. There is no indication of side-bound coordination of the imine nitrogen, as was the case with chelating pyridines²⁴ or benzoate esters.

Crystals suitable for X-ray analysis were obtained for **2.25a** and the resulting structure is shown in Figure 2.8. The complex displays the typical distorted square pyramidal geometry for five-coordinate ruthenium alkylidenes. The Ru–N bond length (2.167(3) Å) is shorter than in the bipyridine precursor **2.3** (2.203(3) Å), consistent with stronger ligand binding. The benzaldimine portion is directed up into the empty quadrant trans to the alkylidene group. This placement of

the phenyl ring maintains the more energetically stable *E*-imine conformation but may result in an unfavorable steric interaction with the RuCl₂ plane (the Cl–Ru–Cl angle is widened to 169.42(4)°).

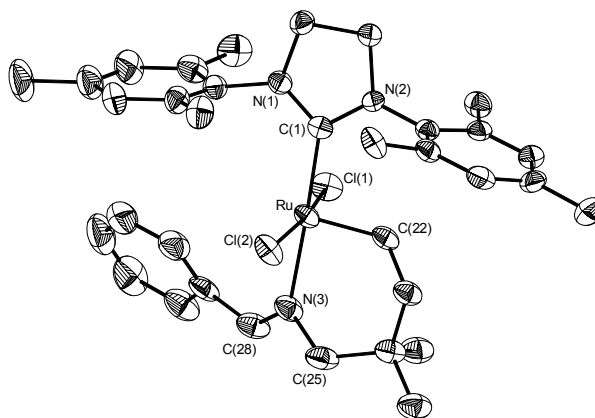


Figure 2.8. Solid state structure of **2.25a** with thermal ellipsoids drawn at 50% probability. Selected bond distances (Å) and angles (deg): Ru–C(1) = 2.052(4), Ru–C(22) = 1.814(4), Ru–N(3) = 2.167(3), Ru–Cl(1) = 2.3905(10), Ru–Cl(2) = 2.3783(10); Cl(1)–Ru–Cl(2) = 169.42(4), C(1)–Ru–N(3) = 176.97(13), C(22)–Ru–N(3) = 87.76(15).

Complexes **2.25a,b** were tested for catalytic activity in the RCM of diethyldiallyl malonate (eq 2.4) and found to be extremely active catalysts. When the reaction was performed at 30 °C with **2.25a**, 90% conversion was reached within 2 min. In fact, **2.25a** is certainly not a latent catalyst and behaves much more like **2.2**, displaying activity below room temperature. Figure 2.9 compares the performance of **2.25a,b** with **2.2** and two derivatives of **2.2**, **2.26**²⁵ and **2.27**²⁶ (Chart 2.6), which were specially engineered to improve the initiation behavior of that family of catalysts. **2.25a** compares favorably to the fast-initiating variants, while **2.25b** shows similar activity to **2.2** in this reaction. In these cases, the initiation behavior is the most likely source of variation since the non-dissociating portion remains the same.

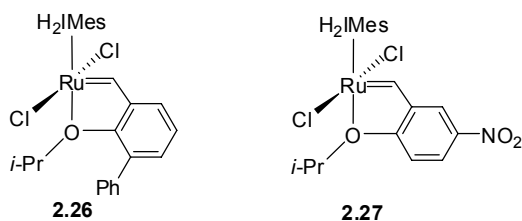


Chart 2.6. Fast-Initiating Variants of **2.2**

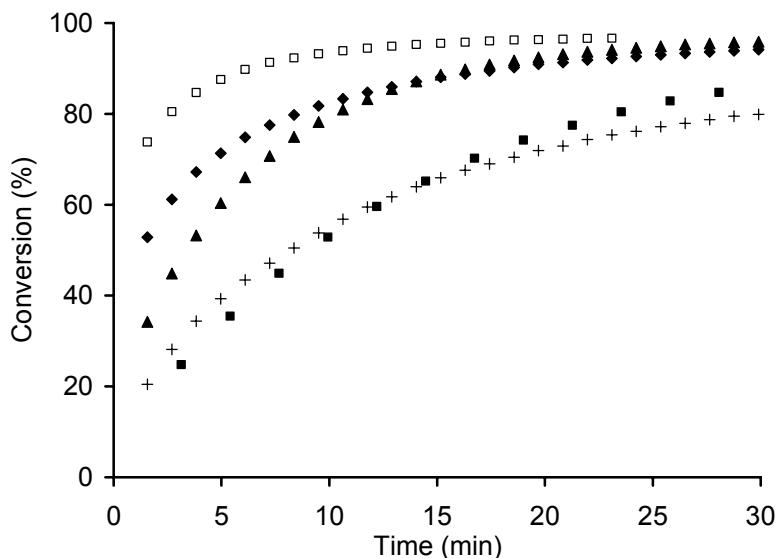


Figure 2.9. Conversion plot for RCM of **2.18** with **2.2** (■), **2.25a** (◆), **2.25b** (+), **2.26** (□), and **2.27** (▲) (2.5 mol%, 10 °C, 0.3 M C₆D₆).

We were interested in whether changing the placement of the imine bond from an exocyclic to an endocyclic position might result in a catalyst with a slower initiation rate. In the course of this study, Slugovc and coworkers reported similar chelated imine frameworks and found that changing the chelate ring size resulted in large differences in catalyst behavior (Chart 2.7).²⁷ In their study, the imine bond was also changed from an exocyclic to an endocyclic placement. To separate these effects, we adapted our catalyst framework to result in an endocyclic imine bond, while maintaining the same six-membered chelate ring size.

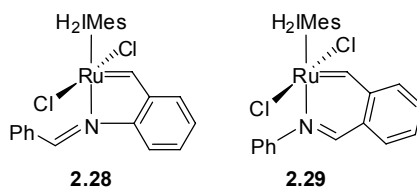
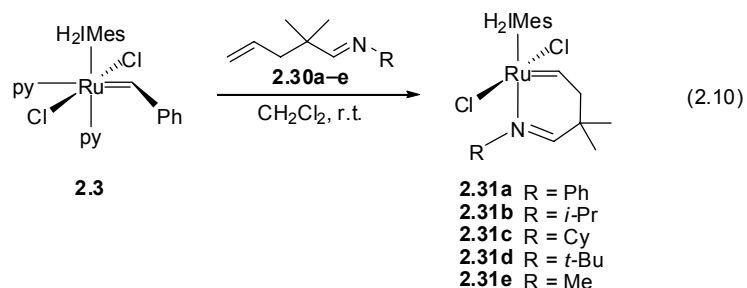


Chart 2.7. Other Chelated Imine-Based Metathesis Catalysts

The imine ligands **2.30a–e** were prepared by condensation of commercially available 2,2-dimethyl-4-pentenal with the corresponding primary amine. The ligands were designed with the gem-dimethyl substituents for two reasons: to stabilize the chelated product by the Thorpe–Ingold effect²⁸ and, more importantly, to prevent formation of enamines, which are known to react to

form catalytically inactive Fischer carbenes.²⁹ The catalysts were synthesized in good yields by reaction of the imine ligands with **2.3** (eq 2.10). The resulting imine-bound compounds **2.31a–e** could be isolated by precipitation on the bench top and easily purified by column chromatography, without decomposition, to give stable pale green solids. Alternatively, the synthesis could be carried out from **2.1**, but this reaction required heating and longer reaction times



The ¹H NMR spectra for **2.31a–e** were similar to those observed for **2.25a,b**. The characteristic downfield alkylidene proton was split into a triplet by coupling to the adjacent methylene protons. Another interesting feature of the spectra is that resonances corresponding to the H₂IMes ligand are affected by the nature of the imine substituent. Groups with small steric profiles like phenyl (**2.31a**) and methyl (**2.31e**) display very sharp ¹H NMR resonances for both the NHC backbone protons and mesityl peaks. For larger groups (e.g. *tert*-butyl, **2.31d**) the ¹H NMR resonances for the NHC protons are significantly broadened. The more sterically demanding groups may hinder free rotation of the NHC causing several protons on the H₂IMes ligand to appear as discrete resonances.³⁰ Though some catalysts show a more symmetric environment than others, there is again no indication of side-bound coordination of the imine nitrogen.

The symmetric nature of the resulting endocyclic imine compounds was confirmed by solid-state structural studies. Crystals suitable for X-ray analysis were obtained for catalysts **2.31a** and **2.31e** and are shown in Figures 2.10 and 2.11, respectively. The Ru–N bond lengths in **2.31a** and **2.31e** (2.149(1) Å and 2.118(3) Å) are shorter than in **2.25a**, suggesting a stronger interaction with the ruthenium for the endocyclic imine donors. The more electron-donating and less sterically demanding methyl substituent displays a shorter Ru–N bond. Additionally the

Cl–Ru–Cl bond angles also reflect differences in the nitrogen substituents, as the bonds in **2.31e** are compressed compared with those in **2.31a** ($162.28(4)^\circ$ vs $167.67(2)^\circ$), likely a result of the lower steric demands of the methyl substituent.

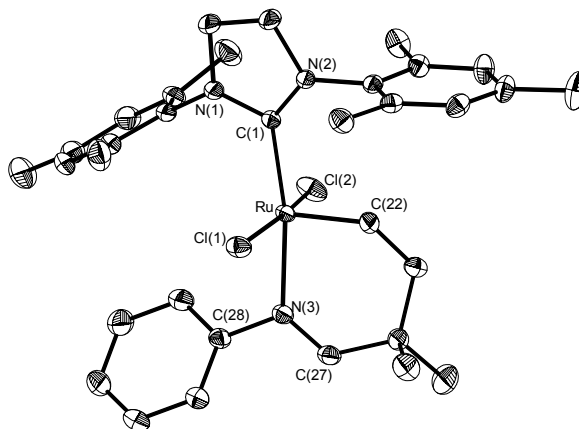


Figure 2.10. Solid-state structure of **2.31a** with thermal ellipsoids drawn at 50% probability. Selected bond distances (Å) and angles (deg): Ru–C(1) = 2.0387(14), Ru–C(22) = 1.8100(15), Ru–N(3) = 2.1488(12), Ru–Cl(1) = 2.3788(4), Ru–Cl(2) = 2.3759(4), C(27)–N(3) = 1.2803(19); Cl(1)–Ru–Cl(2) = 167.674(15), C(1)–Ru–N(3) = 169.94(5), C(22)–Ru–N(3) = 89.67(6).

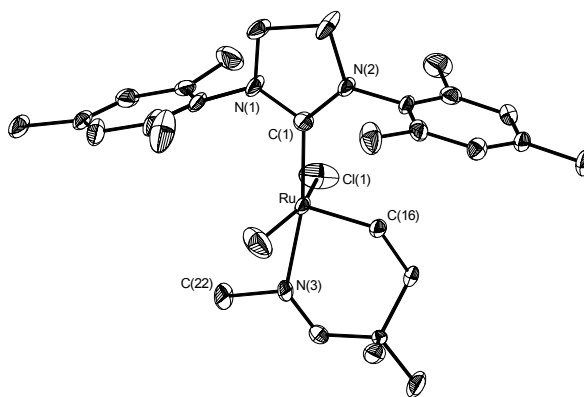


Figure 2.11. Solid-state structure of **2.31e** with thermal ellipsoids drawn at 50% probability. Selected bond distances (Å) and angles (deg): Ru–C(1) = 2.020(3), Ru–C(16) = 1.808(3), Ru–N(3) = 2.118(3), Ru–Cl(1) = 2.3488(9); Cl(1)–Ru–Cl(1)* = 162.28(4), C(1)–Ru–N(3) = 169.66(10), C(16)–Ru–N(3) = 89.71(12) (* symmetry generated).

The imine ligand provides a good handle for IR spectroscopy, in this case one directly involved in the metal binding. The C=N stretching frequencies were measured for the free ligands (**2.30a–e**) and the corresponding ruthenium complexes (**2.31a–e**), and the results are listed in Table 2.1. All catalysts show a decrease in the energy of the C=N stretch indicating a weakening of the bond. This effect could result from π -backbonding from the ruthenium into the

C=N π^* orbital or from binding of the metal forcing the imine out of its ideal conformation, thus weakening the bond. The magnitude of the shift of the $\nu_{\text{C=N}}$ also correlates with the expected strength of the Ru–N interaction. The more tightly bound imine in **2.31e** shows the greatest shift, while the less donating ligand in **2.31a** shows the smallest shift in energy.

Table 2.1. IR Data for Imine C=N Stretch (cm^{-1}) in Free Ligands (**2.30**) and Catalysts (**2.31**)

Imine Substituent	$\nu_{\text{C=N}}$ [2.30]	$\nu_{\text{C=N}}$ [2.31]	$\Delta\nu_{\text{C=N}}$
a , R = Ph	1648.0	1634.3	13.7
b , R = <i>i</i> -Pr	1661.4	1642.6	18.8
c , R = Cy	1662.7	1641.1	21.6
d , R = <i>t</i> -Bu	1665.9	1638.6	27.3
e , R = Me	1670.9	1635.4	35.5

Complexes **2.31a–e** were tested for activity in the RCM of **2.18** at elevated temperature (eq 2.4). Figure 2.13 shows the progress of the reaction when carried out at 40 °C. This reaction is complete (> 95%) within 5–10 min when performed with **2.1** or **2.2**. All complexes examined catalyzed this reaction to completion with an order of activity **2.31a** > **2.31b** > **2.31d** > **2.31c** > **2.31e** (in Figure 2.13 only the first 75 min of reaction time are shown, not the entire reaction profile). These results are consistent with the relative donating ability and the steric demand of the imine substituents: the electron-poor phenyl substituent is the fastest, while the small methyl group shows the slowest reaction. This order of activity also correlates well with the magnitude of the shift in $\nu_{\text{C=N}}$ measured by IR spectroscopy (Table 2.1). To assess the latency of these catalysts, the RCM of **2.18** was studied under standard reaction conditions and referenced to **2.1** and **2.2** (1 mol%, CD_2Cl_2 , 30 °C).³¹ **2.31a** and **2.31e** showed dramatically reduced activity compared to **2.1** and **2.2** near room temperature confirming their latency (see Experimental section).

To evaluate catalyst behavior in polymerization reactions, these complexes were tested in the ROMP of dicyclopentadiene (DCPD) (eq 2.8). Figure 2.13 shows an exotherm graph of DCPD ROMP started at 30 °C for catalysts **2.31a–c**. During the course of the reaction, complete

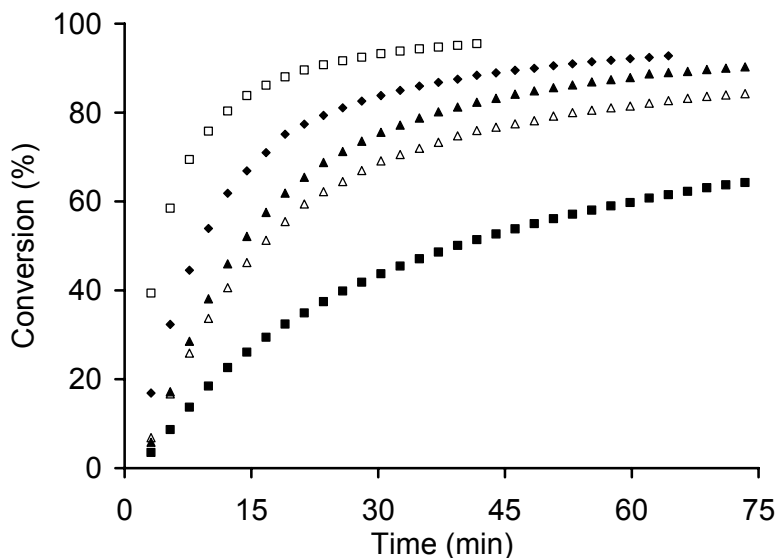


Figure 2.12. Conversion plot for RCM of **2.18** with **2.31a** (□), **2.31b** (◆), **2.31d** (▲), **2.31c** (△), and **2.31e** (■), (2.5 mol%, 40 °C, 0.3 M C₆D₆).

incorporation of DCPD into the polymer was observed. Notable about these graphs is that the trend observed in the RCM data is reflected in the ROMP of DCPD, with the fastest initiating catalyst **2.31a**, showing the shortest time to exotherm. Additionally, the catalysts surveyed show similar peak temperatures, as expected for systems all based on the H₂IMes framework. All catalysts show almost an “on/off” polymerization behavior, without an extended, gradual rise in temperature before the onset of polymerization. This should allow for an educated choice of catalyst to control the time to exotherm while avoiding slow, inefficient polymerization.

The very different initiation behavior of **2.31a** when compared with **2.25a** shows that the relative placement of the imine C=N bond has a large effect on catalyst activity. In this case vastly different activities are observed in spite of the identical chelate ring size. It is possible that the exocyclic imine framework examined here disrupts the Ru–N bonding through a steric interaction with the rest of the catalyst framework. The weakening of the Ru–N bond results in a more efficient initiator and ultimately leads to higher activity. An earlier report ascribed the differences in initiation rates of **2.28** and **2.29** to the varying chelate ring sizes, but the data reported here indicate that the placement of the imine bond has a larger impact on activity than ring size.

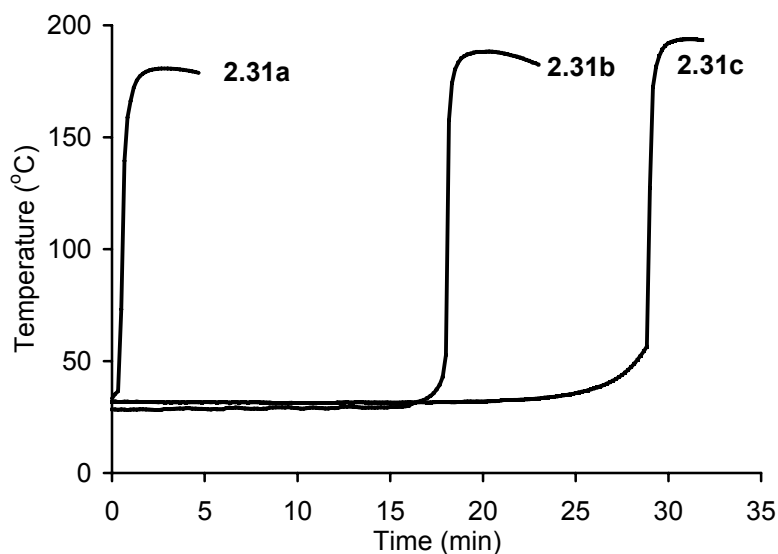
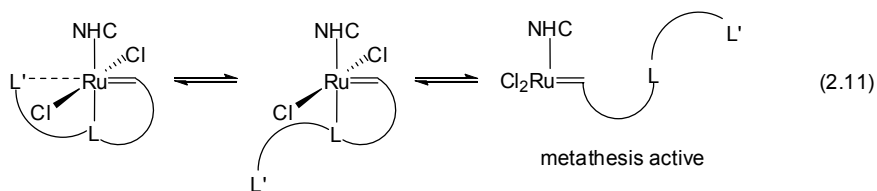


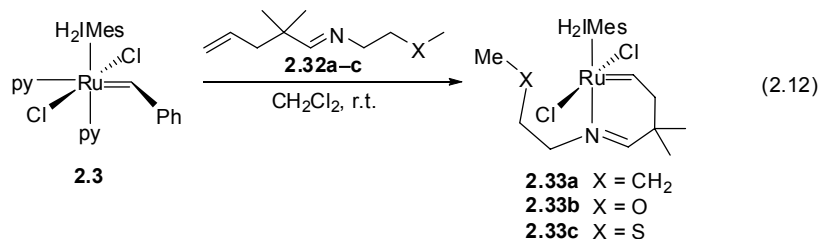
Figure 2.13. Exotherm plot for ROMP of DCPD with **2.31a–c** (30,000:1 M/C, 30 °C).

The development of a simple, modular synthesis of unsaturated imine ligands has also enabled us to examine other related catalyst design motifs. We were interested in synthesizing catalysts that incorporate two potential donor ligands tethered through the alkylidene group. This would set up a 3-point chelate, in which two successive ligand dissociation events must take place before a catalytically active fragment is generated. Potentially, this additional donor could dramatically slow catalyst initiation (eq 2.11). We chose to conserve the imine donor (L) and examine relatively weak third donors (L') in the hope that the additional point of attachment would push the initiation temperatures higher, but retain the high inherent activity of the NHC–Ru framework.



The synthesis of ligands **2.32a–c** was carried out analogously to **2.30a–e** and gave the unsaturated imine ligands containing ether and thioether groups in good yield. The catalyst

synthesis was straightforward starting from **2.3** to give the catalysts **2.33a–c** in good yield (eq 2.12). These catalysts could be easily isolated by precipitation and were quite stable on the benchtop.



The ¹H NMR spectra for **2.32a–c** are consistent with the structures depicted in eq 2.12. The complexes show the characteristic alkylidene protons, which for the thioether compound are shifted slightly upfield (18.45 vs ~18.7 ppm). Most important in these spectra is that the resonance corresponding to the terminal methyl bound to the X donor in **2.33b** and **2.33c** is significantly shifted from that in the free ligand upon complexation to ruthenium, suggesting that the extra donor is binding to the ruthenium center. The terminal methyl resonance in **2.33b** shifts from 3.34 to 2.83 ppm, while the corresponding resonance in **2.33c** shifts from 2.12 to 1.43 ppm. There is almost no shift for the resonance of the terminal methyl group in **2.33a**, where the butyl substituent does not interact with the ruthenium. Somewhat unexpectedly, the resonances corresponding to the H₂IMes ligand are still sharp, suggesting that the extra donor does not inhibit NHC rotation.

The solid-state structure of **2.33c** was determined by X-ray crystallography and is shown in Figure 2.14.³² The complex shows approximate octahedral geometry about the metal center, and the sulfur coordinates to ruthenium trans to the alkylidene. The Ru–S bonding distance (~2.59 Å) is quite long; a search of the Cambridge Crystallographic Database shows that typical Ru–thioether bonds are in the range of 2.3–2.4 Å. The long Ru–S distance in **2.33c** may partially be a result of its placement opposite the strongly trans-influencing alkylidene group. The Ru–N bond distance (~2.17 Å) is longer than that observed in the other imine complexes but may be a consequence of the need to bind a third donor in a five-membered chelate ring. The bond angles

for the pairs of trans ligands ($\text{H}_2\text{IMes-Ru-N}(3) = 177.85(15)^\circ$, $\text{Cl-Ru-Cl} = 172.58(14)^\circ$) are closer to an ideal 180° than in the other square pyramidal ruthenium complexes characterized here.

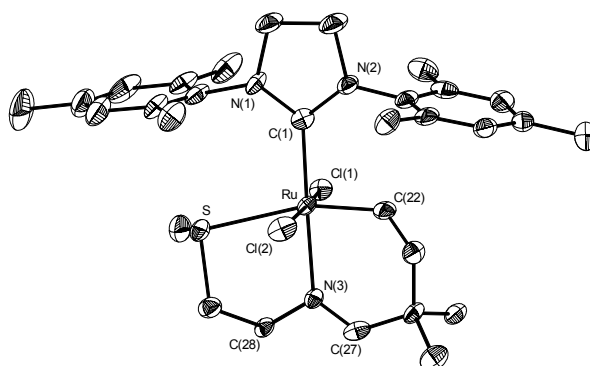


Figure 2.14. Solid-state structure of **2.33c** with thermal ellipsoids drawn at 50% probability. Selected bond distances (Å) and angles (deg): Ru–C(1) = 2.053(4), Ru–C(22) = 1.840(4), Ru–N(3) = 2.185(3), Ru–Cl(1) = 2.4023(10), Ru–Cl(2) = 2.4189(13), Ru–S = 2.5971(12); Cl(1)–Ru–Cl(2) = 172.58(4), C(1)–Ru–N(3) = 177.85(15), C(22)–Ru–N(3) = 83.15(14), C(22)–Ru–S = 163.10(11).

These 3-point chelates were tested in the RCM of **2.18** and found to show activity at elevated temperature (60°C). **2.33a** and **2.33b** show essentially identical activities, which suggests that although the oxygen appears to interact with the ruthenium it does not bind tightly enough to measurably impact the catalysis (Figure 2.15). The sulfur-containing-catalyst **2.33c**, on the other hand, shows much lower activity for RCM, indicating that the thioether has a major impact, which is not unexpected given that sulfur is generally a better ligand for ruthenium than oxygen. NMR data show that precatalyst **2.33c** is still present in significant quantities during the course of the reaction, implying that the complex is not decomposing, but is just a slow initiator. The possibility of sulfur poisoning the catalyst was examined, but reactions carried out in the presence of dimethyl sulfide did not approach the change in rate observed with **2.33c** (see Experimental section). Under these conditions **2.1** and **2.2** catalyze this reaction to completion within 2 min, which highlights the latency of **2.33a–c**. These RCM results suggest that incorporating a third point of attachment can also have a major impact on catalysis but is strongly dependent on the nature of the additional donor.

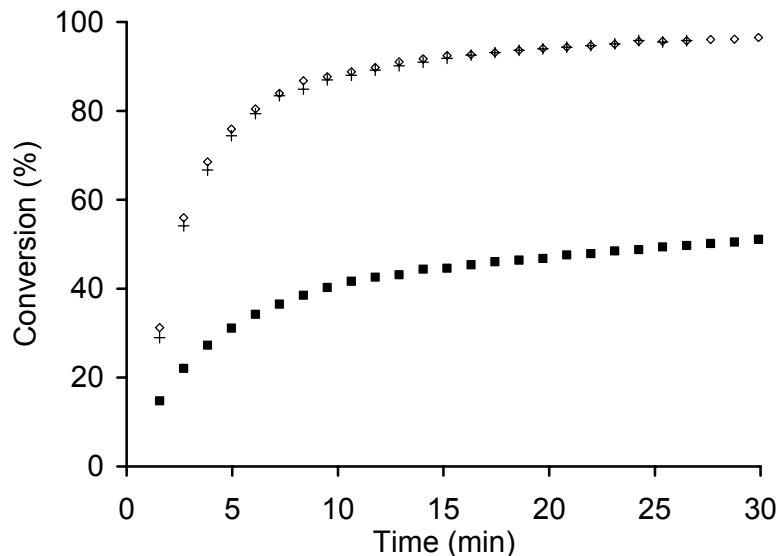


Figure 2.15. Conversion plot for RCM of **2.18** with **2.33a** (+), **2.33b** (◇), and **2.33c** (■) (2.5 mol%, 60 °C, 0.3 M C₆D₆).

Catalysts featuring imine donors chelated through the alkylidene have been synthesized and studied in RCM and ROMP reactions. These catalysts show latent behavior: slow at room temperature but high activity at elevated temperatures. Similar systems also allow access to other strategies, such as the introduction of additional donors, which was shown to have a major impact on catalytic activity. We also examined the effect of relative placement of the imine bond and found that catalysts possessing an exocyclic imine bond resulted in not latent, but fast-initiating metathesis catalysts. The modular synthesis is easily adapted to modification of steric and electronic parameters, allowing for a high degree of tunability of catalyst initiation. These latent catalysts could be useful in a range of high-temperature applications.

Amine chelates

After the successful introduction of imines into latent metathesis catalysts we were interested in whether amine-containing catalysts would show similar behavior. Pyridine and imine donors were preceded, but there were no examples of sp³-hybridized nitrogen centers coordinated to ruthenium-based metathesis catalysts. The introduction of amine ligands would offer further ability to control the donor binding to ruthenium.

Initial attempts to prepare catalysts with chelating 3° amines met with limited success. Reaction of ruthenium precursors with ligands such as allylaniline **2.34** or alkyl substituted **2.35** initially gave new alkylidenes observable by ^1H NMR spectroscopy consistent with the desired products. Over the course of several hours the new products decomposed. These early results suggested that 3° amines were too bulky to coordinate to the ruthenium center and give stable complexes.

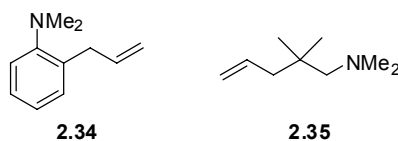
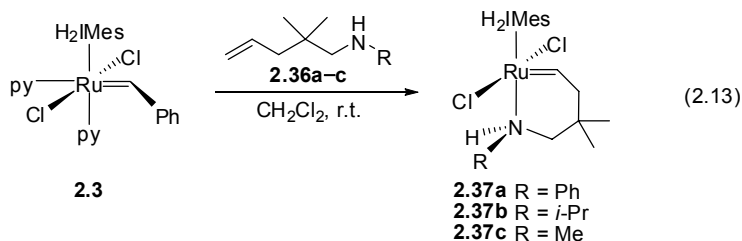


Chart 2.8. 3° Amines Forming Unstable Ru Complexes

2° amines were initially avoided as ligands because the N–H bond held in close proximity to the metal center could potentially be activated, leading to catalyst decomposition. However, when experimentally examined, 2° amines gave much more promising results in catalyst formation than the aforementioned 3° amines. The reaction of **2.3** with amines **2.36a–c** featuring an alkyl tether gave the desired amine-substituted catalysts as light-green solids (eq 2.13). Formation of the phenyl-substituted catalyst **2.37a** occurred more cleanly than the alkyl-substituted **2.37b,c** but all were successfully isolated.



The ^1H NMR spectra of amine-bearing catalysts **2.37** show alkylidene proton resonances that are not substantially different than the corresponding imine catalysts **2.31**.³³ In contrast to the *N*-imine catalysts however, coordination of an sp^3 -hybridized substituted amine nitrogen can create a chiral center in the molecule. This was reflected in the presence of several diastereotopic protons in the ^1H NMR spectra of the new catalysts. In particular, the two protons bound to the methylene alpha to the amine are well resolved. Two broad resonances

corresponding to the aryl mesityl protons are observed; even in the NHC portion, the two faces of the molecule are distinguishable. This also implies that a rotational process (either rotation of the NHC or the appended aryl rings) is slow on the NMR time-scale.

The chiral nature of the catalysts is also clearly evident from the solid-state structure of phenyl-substituted complex **2.37a** (Figure 2.16). This molecule crystallized in a chiral space group with two pairs of enantiomers in the unit cell. The most notable feature of this structure is a lengthening of the Ru–N(3) bond by ~ 0.05 Å when compared to **2.31a**, the corresponding imine catalyst (**2.37a** Ru–N(3) = 2.2060(18) Å, **2.31a** Ru–N(3) = 2.1488(12) Å). The reduction in C–N bond order on moving from imine to amine is also indicated by an elongation of the C–N bond length by ~ 0.15 Å (**2.37a** C(25)–N(3) = 1.435(3) Å, **2.31a** C(27)–N(3) = 1.2803(19) Å). The amine-bound catalyst **2.37a** still maintains the typical square pyramidal geometry, but the *N*-bound phenyl is shifted to one side of the molecule to accommodate the N–H group.

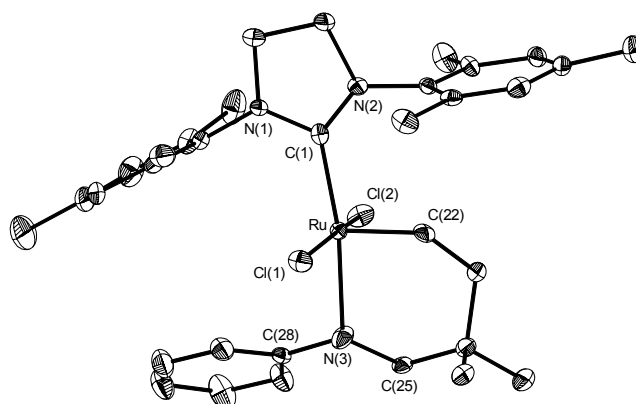


Figure 2.16. Solid-state structure of **2.37a** with thermal ellipsoids drawn at 50% probability. Selected bond distances (Å) and angles (deg): Ru–C(1) = 2.030(2), Ru–C(22) = 1.809(2), Ru–N(3) = 2.2060(18), Ru–Cl(1) = 2.3681(6), Ru–Cl(2) = 2.3914(6), C(28)–N(3) = 1.435(3); Cl(1)–Ru–Cl(2) = 168.67(2), C(1)–Ru–N(3) = 171.21(7), C(22)–Ru–N(3) = 89.78(8).

The new amine-containing catalysts **2.37** were tested in the RCM of **2.18** (eq 2.4) and compared to the corresponding imine-bound catalysts **2.31**. A clear distinction can be made between the aryl-substituted and the alkyl-substituted catalysts. In Figure 2.17 the data for the RCM catalyzed by the phenyl substituted **2.31a** and **2.37a** at 30 °C are shown. The amine-based **2.37a** clearly initiates faster than the imine catalyst. As seen in Figure 2.18, showing RCM data

at 60 °C, for the alkyl-substituted catalysts the situation is reversed. The alkyl amine catalysts **2.37b,c** initiate more slowly than the alkyl imine catalysts **2.31b,c**. We might expect the amines to be uniformly more basic than the imine donors, which would be reflected in the amines being slower initiators, a trend observed for **2.37b,c**. This is not the case for **2.37a** but this effect can be rationalized by examining the amine released. Anilines are known to be significantly less basic than alkyl amines. When catalyst **2.37a** initiates it liberates an aniline that can delocalize the nitrogen lone pair into the aryl ring. This will tend to stabilize the unbound nitrogen form where the lone pair is not interacting with the ruthenium center. It was unexpected that **2.31b** and **2.31c** would show similar activity. The explanation for this is less clear: there must be a fine balance between increased electron density on nitrogen and steric requirements of the amine donors.

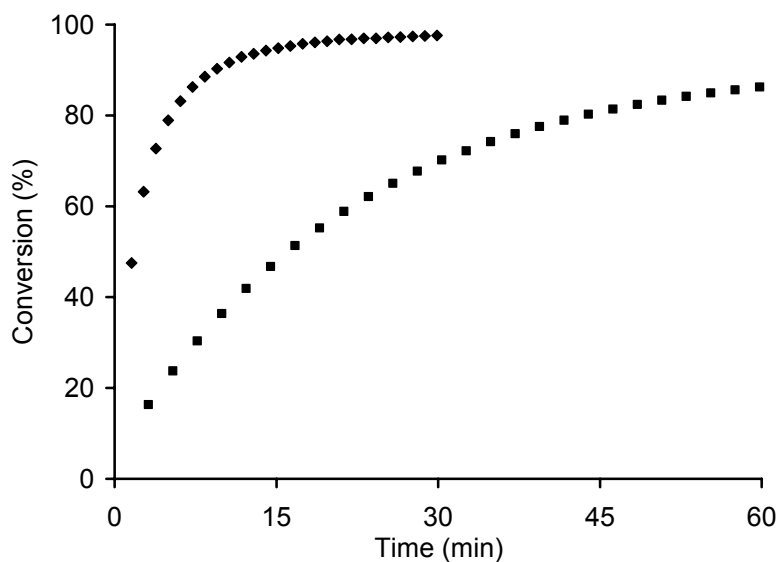


Figure 2.17. Conversion plot for RCM of **2.18** with **2.37a**(◆) and **2.31a** (■) (2.5 mol%, 30 °C, 0.3 M C₆D₆).

Amine ligands containing tethered olefins can bind ruthenium to produce chelated catalysts. Generally, the alkyl amines are better donors than the corresponding imines, but for aryl-substituted nitrogen atoms this trend is reversed. The binding of amines is particularly sensitive to steric bulk, with 3° amines not forming stable complexes with ruthenium. In terms of catalyst synthesis and versatility, the amine ligands seem inferior to the imine frameworks.

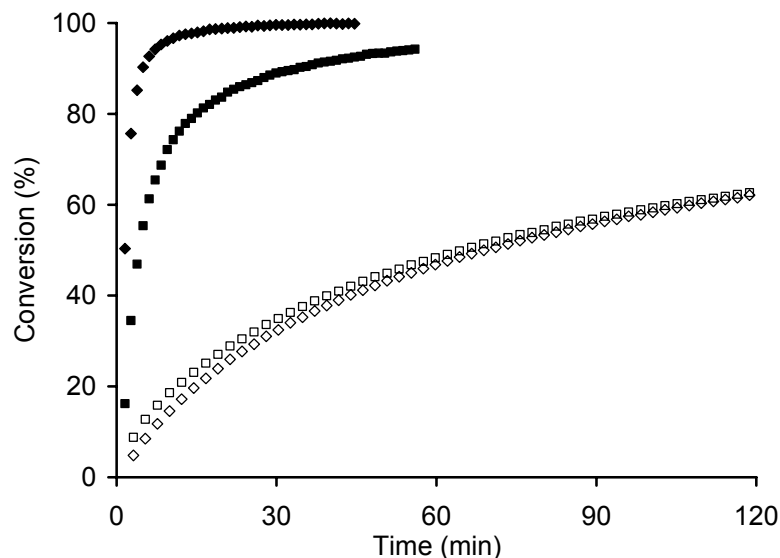


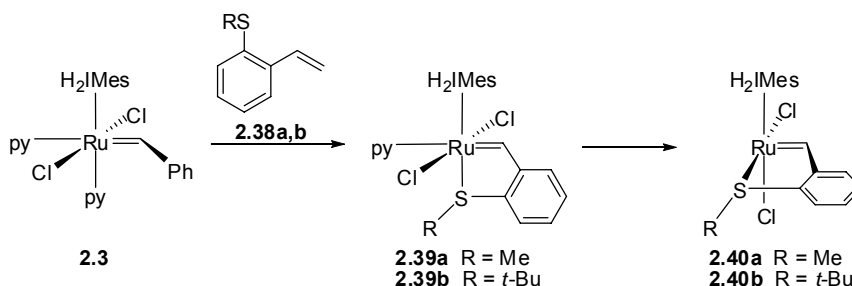
Figure 2.18. Conversion plot for RCM of **2.18** with **2.31b**(◆), **2.31c** (■), **2.37b**(◇), and **2.37c**(□) (2.5 mol%, 60 °C, 0.3 M C₆D₆).

Sulfur chelates

Though there are a number of ruthenium-based metathesis catalysts that feature oxygen donors there are no examples of catalysts with sulfur donors. This is somewhat surprising since sulfur is generally considered a better ligand for ruthenium than oxygen.³⁴ The previously described 3-point chelate **2.33c** showed a definite ruthenium–sulfur interaction, while the corresponding ruthenium–oxygen interaction proved to be much weaker. With this precedent, replacement of the ether ligand in **2.2** with a comparable thioether would likely result in a stable catalyst that might require higher temperatures for initiation.

The synthesis of thioether-substituted styrene ligands **2.38a,b** was easily accomplished by Wittig olefination of the corresponding benzaldehydes. The reaction of catalyst **2.3** with styrenes **2.38a,b** resulted in the fast formation of new ruthenium complexes (Scheme 2.3). In the case of the methyl-substituted styrene **2.38a**, a new complex **2.39a** formed initially (¹H NMR benzylidene: 17.29 ppm), but was quickly consumed to produce a second complex **2.40** (¹H NMR benzylidene: 17.01 ppm). Based on previous experience with the pyridine chelates, the structures of the two products were hypothesized to be side-bound and bottom-bound isomers.

With thiomethyl substitution the intermediate structure could not be cleanly isolated as the rate of isomerization was competitive with complex formation. By changing the sulfur substituent to *tert*-butyl, the isomerization could be retarded and it was possible to isolate the bottom-bound complex **2.39b** after the initial olefin metathesis step.



Scheme 2.3. Preparation of Thioether Complexes

Examination of the ^1H NMR spectra of the new complexes **2.39a,b** and **2.40a,b** supported the hypothesis that they were C_s and C_1 isomers. The thermodynamic products **2.40** show many of the same features as the C_1 pyridine complex **2.21**. Specifically, a complete desymmetrization of the H_2IMes ligand results in separate resonances for the six mesityl methyl groups, and a complicated NHC backbone region. Consistent with its higher symmetry, the ^1H NMR spectrum for **2.39b** resembles that obtained for ether-bound catalyst **2.2**. Two sets of resonances for the mesityl methyl groups and a single resonance for the four backbone protons are observed. The ^1H NMR spectrum for **2.39b** also revealed that the catalyst maintained one equivalent of pyridine. The additional pyridine ligand is presumably bound trans to the benzylidene giving an octahedral complex. Catalyst **2.39b** is the only example of a ruthenium complex with a chelating alkylidene, in which pyridine from **2.3** was not completely displaced.

X-ray analysis of crystals obtained of the *tert*-butyl-substituted catalysts **2.39b** and **2.40b** (Figure 2.19 and Figure 2.20) confirmed the structures as the C_s and C_1 complexes. In the unit cell for **2.39b**, two distinct molecules were observed, one with a coordinated pyridine as observed in solution and one in which the pyridine has dissociated. Apart from the lack of pyridine the two molecules are very similar, so only the example with pyridine will be discussed. The long Ru–N bond distance (2.353(2) Å) is very similar to that observed in catalyst **2.3** (2.348(7) Å) and

suggests that the pyridine ligand trans to the alkylidene is not tightly bound. This effect is confirmed by the partial loss of pyridine from **2.39b** upon crystallization. Again, as expected from the strong trans influencing NHC ligand, the Ru–S distance in **2.39b** (2.4446(7) Å) is significantly longer than the Ru–S distance in **2.40b** (2.355(2) Å). Both distances are much shorter than the Ru–S distance in **2.33c** (2.5971(12) Å). The difference in bond length between the two isomers is even greater than that observed in the two pyridine isomers **2.20a** and **2.21** and suggests a potentially large difference in reactivity with olefins. Side-bound catalyst **2.40b** displays a shortening (by ~0.05 Å) of several other bonds including Ru–C(1) and Ru–C(28). Significant deviations from an ideal square pyramidal geometry are also observed. The chloride located trans to the NHC is pushed far back into the empty quadrant ($C(1)–Ru–Cl(1) = 148.2(2)^\circ$).

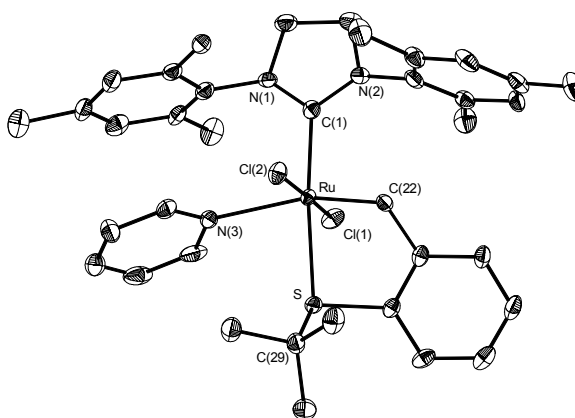


Figure 2.19. Solid-state structure of **2.39b** with thermal ellipsoids drawn at 50% probability. Selected bond distances (Å) and angles (deg): Ru–C(1) = 2.076(3), Ru–C(22) = 1.859(3), Ru–S = 2.4446(7), Ru–N(3) = 2.353(2), Ru–Cl(1) = 2.3943(7), Ru–Cl(2) = 2.4135(7); Cl(1)–Ru–Cl(2) = 176.27(3), C(1)–Ru–S = 165.31(8), C(22)–Ru–N(3) = 160.84(10), C(22)–Ru–S = 82.75(9).

To gain more insight into these two distinct binding modes, the C_s to C_1 isomerization process was studied in more detail (eq 2.14). The reaction showed a definite solvent dependence; **2.39b** isomerized to **2.40b** much more quickly in polar, chlorinated solvents than in benzene. Unlike the pyridine complexes **2.20b** and **2.21**, the two thioether isomers do not seem

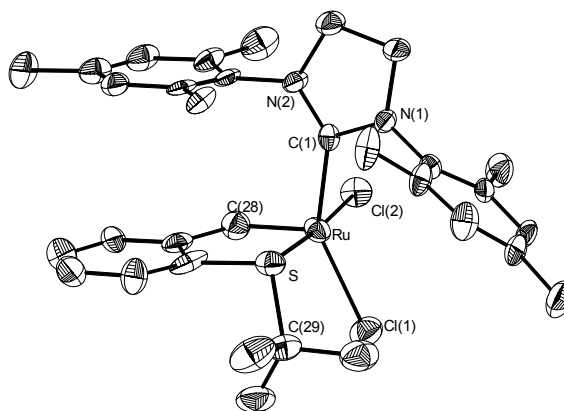
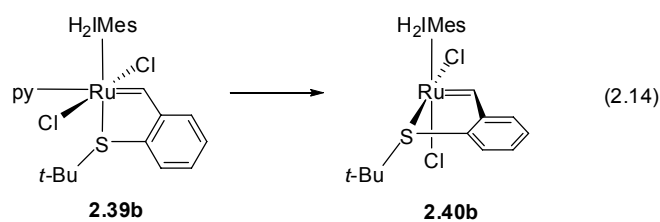


Figure 2.20. Solid-state structure of **2.40b** with thermal ellipsoids drawn at 50% probability. Selected bond distances (Å) and angles (deg): Ru–C(1) = 2.007(7), Ru–C(28) = 1.757(8), Ru–S = 2.355(2), Ru–Cl(1) = 2.371(2), Ru–Cl(2) = 2.391(2); Cl(1)–Ru–Cl(2) = 86.20(8), C(1)–Ru–S = 93.4(2), C(28)–Ru–S = 84.0(3), C(1)–Ru–Cl(1) = 148.2(2), C(1)–Ru–Cl(2) = 85.7(2), Cl(2)–Ru–S = 172.40(8).

to be in equilibrium; **2.40b** was not observed to revert to **2.39b**, regardless of solvent. By performing the reaction in CDCl_3 , ^1H NMR spectroscopy could be used to monitor the isomerization process. The reaction was found to be first order with a half-life of approximately 20 min at 55 °C. By varying the temperature and performing an Eyring analysis, the activation parameters $\Delta H^\ddagger = 15(3)$ kcal/mol and $\Delta S^\ddagger = -17(10)$ e.u. could be obtained. These parameters are consistent with an intramolecular rearrangement process.³⁵



The relative stability of these thioether complexes was related to their catalytic efficiency. As observed with the isomeric pyridine catalysts, the C_1 catalysts **2.40a,b** performed the RCM of **2.18** slowly (Table 2.2). When performed at 100 °C, methyl-substituted **2.40a** (32% after 1 d) was much less active than *tert*-butyl substituted **2.40b** (92% in 6 h). The catalytic behavior of the C_s isomer **2.39b** was very dependent on the catalytic conditions. When performed in C_6D_6 at 60 °C, the reaction was complete within 3 hours, but at the same temperature in TCE-d_2 , only 4% conversion was observed within 24 h. The source of the poor conversion is competitive

isomerization occurring in the chlorinated solvent. In TCE- d_2 , **2.39b** isomerizes to the less active **2.40b** faster than it can perform the metathesis and so lower conversion is observed. This effect was not observed for the pyridine chelates because the isomerization was significantly slower than the metathesis reaction.

Table 2.2. Conversion data for RCM of **2.18** with thioether catalysts (5 mol%).

Catalyst	Solvent	Temperature (°C)	Conversion (Time)
2.40a	TCE- d_2	100	32% (1 d)
2.40b	TCE- d_2	100	92% (6 h) 100% (1 d)
2.40b	TCE- d_2	60	13% (1 d)
2.39b	TCE- d_2	60	4% (1 d)
2.39b	C ₆ D ₆	60	95% (3 h)

It was gratifying to observe that, as predicted, the sulfur-containing catalysts showed lower activity than oxygen-containing systems. The isomerization of bottom-bound **2.39** to side-bound **2.40** is interesting, particularly since this process is unknown for the ether analogs. This isomerization again highlights the relatively small gap in energy between the bottom-bound and side-bound geometries. The wider implications of this small energy gap are unclear but these observations may further confuse our understanding of potential olefin binding geometries. Unlike the pyridine chelates, the thioether isomers do not appear to be in equilibrium; the C_1 form lies energetically downhill.

Conclusions

The studies presented in this chapter show that chelating a neutral donor ligand through the alkylidene portion is an effective method for controlling initiation and designing latent olefin metathesis catalysts. The incorporation of weak donors, such as pyridines and imines, is particularly effective. Stronger ligands, such as phosphines, are likely to re-coordinate during the reaction and will slow propagation as well as initiation. The use of imines as neutral donors resulted in the most effective framework since they had a simple modular synthesis that allowed

for the preparation of numerous catalysts with tunable initiation behavior. Subtle changes, such as the relative placement of the imine bond (exocyclic vs endocyclic), resulted in major differences in catalytic performance. In two instances (pyridines and thioethers) isomeric products were formed with the neutral donor binding in both bottom-bound and side-bound geometries. The rules governing this process are not completely understood but in these cases the two isomers seem to be very close in energy. The presence of two isomers may have important implications on olefin binding geometry. One key advantage of these chelated alkylidene complexes is that phosphine-free systems can be prepared that are extremely stable and easy to handle.

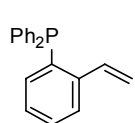
Experimental

Materials and Methods. All manipulations involving organometallic complexes (apart from chromatography) were performed using a combination of glovebox and Schlenk techniques under a nitrogen atmosphere. Unless otherwise indicated, all compounds were purchased from Aldrich, Alfa-Aesar, or Strem and used as received. Anhydrous solvents (purchased from Fisher) were rigorously degassed and obtained via elution through a solvent column drying system.³⁶ Deuterated solvents were purchased from Cambridge Isotope Laboratories, distilled from CaH₂ into a Schlenk tube, and degassed by freeze, pump, thaw cycles 3 times. Silica gel for the purification of organometallic complexes was obtained from TSI Scientific, Cambridge, MA (60 Å, pH 6.5–7.0). Catalysts **2.1** and **2.2** were received as gifts from Materia, Inc. **2.3**, **2.26**, **2.27**, **2.34**,³⁷ **2.35**,³⁸ **2.36a**,³⁹ **2.41**,⁴⁰ 4-pentenyldiphenylphosphine,⁴¹ and 2-(3-butenyl)pyridines were prepared according to literature procedures. Diethyldiallyl malonate (**2.18**) was purchased from Aldrich and distilled before use.

Methods. NMR spectra were recorded on Varian Inova 500 and Mercury 300 spectrometers. ¹H NMR chemical shifts are reported in ppm relative to SiMe₄ ($\delta = 0$) and referenced internally with respect to the protio solvent impurity. ¹³C NMR spectra were referenced internally with respect to the solvent resonance. ³¹P NMR spectra were referenced using H₃PO₄ ($\delta = 0$) as an external

standard. NMR reaction temperatures were determined by measuring the peak separations of an ethylene glycol or methanol standard. IR spectra were recorded on a Perkin-Elmer Paragon 1000 spectrophotometer.

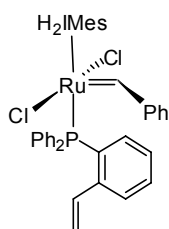
Characterization of styrene 2.11a. The styrene was prepared according to known procedure.



2.11a

^1H NMR (CDCl_3 , 300 MHz, δ): 7.59 (m, 2 H, Aryl H), 7.42–7.20 (m, 15 H, Aryl H, $\text{ArCH}=\text{CH}_2$), 5.97 (dd, $J = 13.2, 1.5$ Hz, 1 H, $\text{ArCH}=\text{CH}_2$), 4.96 (dd, $J = 6.3, 1.5$ Hz, 1 H, $\text{ArCH}=\text{CH}_2$). $^{31}\text{P}\{^1\text{H}\}$ NMR (CDCl_3 , 121 MHz, δ): 44.19.

Synthesis of 2.12a. In the glove box, a flask was charged with **2.3** (25 mg, 0.034 mmol) and

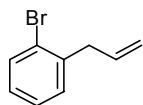


2.12a

toluene (5 mL). Styrene **2.11a** (10 mg, 0.039 mmol) was added and the reaction allowed to stir at 40 °C for 30 min before the volatiles were removed under vacuum. The residue was redissolved in toluene (5 mL) and stirred 30 min at 40 °C before the volatiles were again removed. This procedure was repeated a third time. The residue was washed with pentane, dried under vacuum, and

the resulting light brown solid characterized by NMR spectroscopy as **2.12a**. ^1H NMR (CD_2Cl_2 , 300 MHz, δ): 19.07 (s, $\text{Ru}=\text{CH}$). $^{31}\text{P}\{^1\text{H}\}$ NMR (CD_2Cl_2 , 121 MHz, δ): 44.19.

Synthesis of 2-bromoallylbenzene. CuI (0.500 g, 2.62 mmol) and 2,2'-bipyridine (0.404 g, 2.59 mmol) were dissolved in C_6H_6 (10 mL) in a flame-dried flask. 2-bromobenzyl

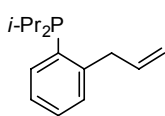


bromide (6.36 g, 25.4 mmol) was added and the mixture cooled to 0 °C.

Vinylmagnesium bromide (1.0 M in THF, 40 mL, 40 mmol) was added quickly and the color changed to deep red. The reaction was stirred 1.5 h at 0 °C and 2.5 h at r.t. The reaction was quenched by addition of NH_4Cl (s), Et_2O (50 mL), H_2O (50 mL) and conc. NH_4OH (5 mL) and stirred 30 min. The layers were separated and the aqueous layer extracted with Et_2O . The combined organics were washed sequentially with H_2O , 1N HCl , NaHCO_3 (sat.), and brine then dried over MgSO_4 . The volatiles were removed to give an orange liquid that was purified by column chromatography (2.5% EtOAc /hexanes, $R_f \sim 0.75$) to give the desired product as a

colorless liquid. Yield 3.133 g (63%). ^1H NMR (CDCl_3 , 300 MHz, δ): 7.69 (m, 1 H, Aryl H), 7.32–7.04 (m, 3 H, Aryl H), 5.98 (m, 1H, $\text{CH}_2=\text{CHCH}_2$), 5.15–5.03 (m, 2 H, $\text{CH}_2=\text{CH}$), 3.52 (dt, $J = 6.3$, 1.8 Hz, 2 H, CHCH_2Ph).

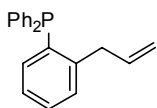
Synthesis of 2-(diisopropylphosphino)allylbenzene (2.14a). 2-bromoallylbenzene (1.37 g,



2.14a

7.96 mmol) was dissolved in Et_2O (20 mL) in a flame-dried flask and cooled to 0 °C. *n*-BuLi (1.6 M in hexane, 5.2 mL, 8.3 mmol) was added dropwise and the solution stirred 45 min. *i*-Pr₂PCl (1.26 mL, 1.21 g, 7.92 mmol) was added to the solution upon which the color changed to milky white and a precipitate formed. The mixture was stirred for 30 min warming to r.t., after which the reaction was quenched with NH_4Cl (sat.) and H_2O and the layers separated. The aqueous layer was extracted 2x with Et_2O , the combined organics washed with brine and dried over MgSO_4 . The solution was concentrated to give a slightly yellow liquid that was purified by column chromatography (5% EtOAc/hexanes, $R_f = 0.27$) to give **2.14a** as a clear liquid. Yield: 0.761 g (39%). ^1H NMR (CDCl_3 , 300 MHz, δ): 7.4–7.1 (m, 4 H, Aryl H), 6.03–5.89 (m, 1 H, $\text{CH}_2=\text{CHCH}_2$), 5.03–4.89 (m, 2 H, $\text{CH}_2=\text{CH}$), 3.77 (m, 2 H, CHCH_2Ph), 2.06 (sept. d, $J = 6.9$, 2.4 Hz, 2 H, PCHMe_2), 1.12 (d, $J = 6.3$ Hz, 3 H, PCHMe_2), 1.07 (d, $J = 6.3$ Hz, 3 H, PCHMe_2), 0.88 (d, $J = 6.3$ Hz, 3 H, PCHMe_2), 0.84 (d, $J = 6.3$ Hz, 3 H, PCHMe_2). ^{31}P NMR (CDCl_3 , 121 MHz, δ): -5.97 (s).

Synthesis of 2-(diphenylphosphine)allylbenzene (2.14b). 2-bromoallylbenzene (1.35 g, 7.8

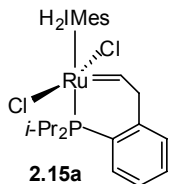


2.14b

mmol) was dissolved in Et_2O (30 mL) in a flame-dried flask and cooled to 0 °C. *n*-BuLi (1.4 M in hexane, 6.0 mL, 8.4 mmol) was added dropwise and the solution stirred 45 min. Ph_2PCl (1.44 mL, 1.71 g, 7.8 mmol) was added to the solution, upon which the color changed to dark red, and the reaction stirred for 1 h at 0 °C. The reaction was quenched with NH_4Cl (sat.) and H_2O and the layers separated. The aqueous layer was extracted 2x with Et_2O , the combined organics washed with brine and dried over MgSO_4 . The solution was concentrated to give a slightly yellow liquid that was purified by column chromatography (5% EtOAc/hexanes, $R_f = 0.34$) to give **2.14b** as a pale yellow liquid. Yield:

1.355 g (57%). ^1H NMR (C_6D_6 , 300 MHz, δ): 7.4–6.9 (m, 14 H, Aryl H), 5.95–5.80 (m, 1 H, $\text{CH}_2=\text{CHCH}_2$), 5.00–4.90 (m, 2 H, $\text{CH}_2=\text{CH}$), 3.77 (m, 2 H, CHCH_2Ph). ^{31}P NMR (C_6D_6 , 121 MHz, δ): -14.51 (s).

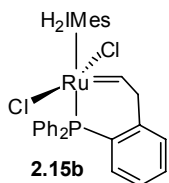
Synthesis of catalyst 2.15a. In the glove box, a flask was charged with **2.3** (158 mg, 0.22 mmol) and CH_2Cl_2 (5 mL). Phosphine **2.15a** (58 mg, 0.21 mmol) was then added



via syringe and the reaction allowed to stir for 30 minutes before the volatiles were removed under vacuum. The solid was purified by column chromatography (Et_2O /pentane, 5% then 50%) and dried under vacuum to give **2.15a** (79 mg,

0.11 mmol) as a green-brown solid upon drying. Yield: 52%. ^1H NMR (CD_2Cl_2 , 300 MHz, δ): 18.27 (pseudo quartet, $J = 3.6$ Hz, 1 H, $\text{Ru}=\text{CHCH}_2$), 7.36–7.09 (m, 4 H, Aryl H), 6.99 (s, 2 H, Mes), 6.93 (s, 2 H, Mes), 4.14–3.96 (m, 4 H, $\text{NCH}_2\text{CH}_2\text{N}$), 3.08 (d, $J = 3.0$ Hz, 2 H, $\text{Ru}=\text{CHCH}_2$), 2.56 (s, 6 H, $\text{Mes}-\text{CH}_3$), 2.41 (s, 6 H, $\text{Mes}-\text{CH}_3$), 2.37 (s, 3 H, $\text{Mes}-\text{CH}_3$), 2.29 (s, 3 H, $\text{Mes}-\text{CH}_3$), 2.16 (m, 2 H, PCHMe_2), 0.87 (d, $J = 7.5$ Hz, 3 H, PCHMe_2), 0.83 (d, $J = 7.2$ Hz, 3 H, PCHMe_2), 0.33 (d, $J = 7.2$ Hz, 3 H, PCHMe_2), 0.27 (d, $J = 6.6$ Hz, 3 H, PCHMe_2). $^{31}\text{P}\{^1\text{H}\}$ NMR (CD_2Cl_2 , 121 MHz, δ): 61.85. $^{13}\text{C}\{^1\text{H}\}$ NMR (CD_2Cl_2 , 125 MHz, δ): 321.31 (d) ($\text{Ru}=\text{CH}$), 221.06 ($\text{Ru}-\text{C}(\text{N})_2$), 144–126 (numerous aryl peaks), 82.86, 60.19 (d), 51.84, 51.61, 21.53, 21.24, 21.21, 21.09, 20.12, 19.17, 18.78, 17.95, 17.35, 17.25. HRMS–FAB (m/z): $[\text{M}]^+$ calcd for $\text{C}_{35}\text{H}_{47}\text{Cl}_2\text{N}_2\text{PRu}$, 698.1898; found, 698.1927.

Synthesis of catalyst 2.15b. In the glove box, a flask was charged with **2.3** (110 mg, 0.15 mmol) and toluene (5 mL). Phosphine **2.14b** (64 mg, 0.21 mmol) was then

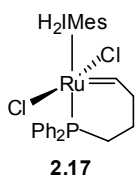


added via syringe and the reaction was heated to 40 °C for 30 min before the volatiles were removed under vacuum. The residue was redissolved in toluene (5 mL) and stirred 30 min at 40 °C before the volatiles were again removed. This

procedure was repeated a third time. The resulting residue was purified by column chromatography (Et_2O /pentane, 5% then 50%) and dried under vacuum to give catalyst **2.15b** (63 mg, 0.0082 mmol) as a light brown solid upon drying. Yield: 54%. ^1H NMR (CD_2Cl_2 , 300 MHz,

δ): 17.99 (pseudo quartet, $J = 3.0$ Hz, 1 H, Ru=CHCH₂), 7.4–6.9 (m, 18 H, Aryl H), 4.07 (s, 4 H, NCH₂CH₂N), 2.88 (d, $J = 3.6$ Hz, 2 H, Ru=CHCH₂), 2.54 (br s, 6 H, Mes–CH₃), 2.36 (br s, 12 H, Mes–CH₃). ³¹P{¹H} NMR (CD₂Cl₂, 121 MHz, δ): 37.80. ¹³C{¹H} NMR (CD₂Cl₂, 125 MHz, δ): 327.90 (d) (Ru=CH), 218.90 (Ru–C(N)₂), 144–126 (numerous aryl peaks), 62.38 (d), 52.12, 51.78, 21.49, 21.35, 20.24, 18.72. HRMS–FAB (m/z): [M]⁺ calcd for C₄₁H₄₃Cl₂N₂PRu, 766.1585; found, 766.1583.

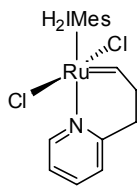
Synthesis of catalyst 2.17. In the glove box, a flask was charged with **2.3** (127 mg, 0.17 mmol)



and CH₂Cl₂ (5 mL). (4-pentenyl)diphenylphosphine (49 mg, 0.19 mmol) was then added via syringe and the reaction allowed to stir at r.t. for 30 min. The volatiles were removed under vacuum and the residue was washed with pentane (2 x 2 mL).

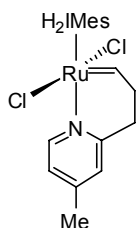
The solid was redissolved in CH₂Cl₂ (5 mL) and heated to 40 °C for 12h, after which volatiles were removed under vacuum. The solid was purified by column chromatography (Et₂O/pentane, 5% then 25%) and dried under vacuum to give **2.17** (59 mg, 0.082 mmol) as a light brown solid upon drying. Yield: 47%. ¹H NMR (CD₂Cl₂, 300 MHz, δ): 18.60 (td, $J = 6.3$ Hz, 1.8 Hz, 1 H, Ru=CHCH₂), 7.30 (m, 2 H, PPh₂), 7.18 (m, 4 H, PPh₂), 6.97 (s, 4 H, Mes), 6.89 (m, 4 H, PPh₂), 4.07 (m, 4 H, NCH₂CH₂N), 2.79 (q, $J = 6.3$ Hz, 2 H, Ru=CHCH₂CH₂), 2.53 (s, 6 H, Mes–CH₃), 2.39 (s, 6 H, Mes–CH₃), 2.35 (s, 6 H, Mes–CH₃), 2.30 (m, 2 H, CH₂CH₂PPh₂), 1.53 (m, 2 H, CH₂CH₂CH₂PPh₂). ³¹P{¹H} NMR (CD₂Cl₂, 121 MHz, δ): 45.49. ¹³C{¹H} NMR (CD₂Cl₂, 125 MHz, δ): 327.24 (d) (Ru=CH), 221.10 (Ru–C(N)₂), 139.42, 138.82, 138.51, 137.85, 137.77, 134.82, 133.53 (d), 132.88, 132.56, 129.98, 129.78 (d), 128.25 (d), 53.38 (d), 52.29, 51.37, 22.23, 21.98, 21.60, 21.38, 20.24, 18.98, 18.94. HRMS–FAB (m/z): [M]⁺ calcd for C₃₇H₄₃Cl₂N₂PRu, 718.1585; found, 718.1550.

Synthesis of catalyst 2.20a. *Method A:* A flask was charged with **2.1** (10.0 g, 11.8 mmol). The flask was capped, sparged with Ar for 15 min, and charged with CH₂Cl₂ (118 mL). 2-(3-Butenyl)pyridine (2.4 g, 17.7 mmol) was then added via syringe and the reaction mixture was

**2.20a**

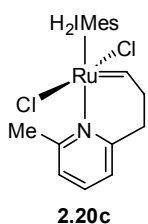
heated to 40 °C for 6 h. The reaction mixture was concentrated to dryness and the residue triturated with degassed, chilled MeOH. The solid was collected on a frit and washed with chilled MeOH (2 x 25 mL) to give **2.20a** (5.6 g, 9.4 mmol) as a pale green solid upon drying. Yield: 80%. *Method B:* In the glove box a vial was charged with 2-(3-butenyl)pyridine (24 mg, 0.18 mmol) and CH₂Cl₂ (2 mL). Complex **2.3** (86 mg, 0.12 mmol) was then added as a solid and the reaction allowed to stir at r.t. for 30 min. The volatiles were removed under vacuum and the residue triturated with hexanes. The solid was collected, washed with hexanes (2 x 1 mL) and dried under vacuum to give **2.20a** (60 mg, 0.10 mmol) as a pale green solid upon drying. Yield: 85%. ¹H NMR (CD₂Cl₂, 300 MHz, δ): 18.46 (t, *J* = 2.7 Hz, 1 H, Ru=CHCH₂), 7.64 (d, *J* = 4.8 Hz, 1 H, Py), 7.52 (t, *J* = 7.2 Hz, 1 H, Py), 7.14 (d, *J* = 7.8 Hz, 1 H, Py), 7.07 (s, 4 H, Mes), 6.99 (t, *J* = 6.9 Hz, 1 H, Py), 4.09 (s, 4 H, NCH₂CH₂N), 3.55 (t, *J* = 5.7 Hz, 2 H, CH₂-Py), 2.50 (s, 12 H, Mes-CH₃), 2.41 (s, 6 H, Mes-CH₃), 1.70 (m, 2 H, Ru=CHCH₂). ¹³C{¹H} NMR (CD₂Cl₂, 125 MHz, δ): 339.18 (Ru=CH), 216.52 (Ru-C(N)₂), 162.64, 158.34, 149.54, 138.96, 138.83, 136.96, 129.60, 124.51, 121.82, 54.45, 51.92, 34.30, 21.32, 19.58.

Synthesis of catalyst 2.20b. In the glove box, a flask was charged with 2-(3-butenyl)-4-methylpyridine (40 mg, 0.27 mmol) and CH₂Cl₂ (5 mL). Complex **2.3** (114 mg, 0.16 mmol) was then added as a solid and the reaction allowed to stir at r.t. for 30 min. The volatiles were removed under vacuum and the residue was redissolved in C₆H₆ (1 mL) and precipitated with pentane (10 mL). The solid was collected, washed with pentane (3 x 5 mL) and dried under vacuum to give **2.20b** (80 mg, 0.13 mmol) as a

**2.20b**

light brown solid upon drying. Yield: 84%. ¹H NMR (CD₂Cl₂, 300 MHz, δ): 18.44 (t, *J* = 3.3 Hz, 1 H, Ru=CHCH₂), 7.42 (d, *J* = 5.7 Hz, 1 H, Py), 7.02 (s, 4 H, Mes), 6.95 (s, 1 H, Py), 6.80 (d, *J* = 4.2 Hz, 1 H, Py), 4.06 (s, 4 H, NCH₂CH₂N), 3.46 (t, *J* = 6.0 Hz, 2 H, CH₂Py), 2.45 (s, 12 H, Mes-CH₃), 2.37 (s, 6 H, Mes-CH₃), 2.27 (s, 3 H, Py-CH₃), 1.66 (m, 2 H, Ru=CHCH₂). ¹³C{¹H} NMR (CD₂Cl₂, 125 MHz, δ): 339.16 (Ru=CH), 216.91 (Ru-C(N)₂), 161.97, 148.96, 148.87, 138.99, 138.83, 129.63, 125.43, 122.98, 54.62, 51.95, 34.13, 21.35, 21.01, 19.64.

Synthesis of catalyst 2.20c. In the glove box, a flask was charged with 2-(3-butenyl)-6-



methylpyridine (50 mg, 0.34 mmol) and CH_2Cl_2 (5 mL). Complex **2.3** (98 mg, 0.14 mmol) was then added as a solid and the reaction allowed to stir at r.t. for 30 min.

The volatiles were removed under vacuum and the residue was redissolved in C_6H_6 (1 mL) and precipitated with pentane (10 mL). The solid was collected,

washed with pentane (3 x 5 mL) and dried under vacuum to give **2.20c** (57 mg, 0.094 mmol) as a

light brown solid upon drying. Yield: 69%. ^1H NMR (CD_2Cl_2 , 300 MHz, δ): 18.33 (t, J = 3.6 Hz, 1

H, $\text{Ru}=\text{CHCH}_2$), 7.34 (t, J = 7.5 Hz, 1 H, Py), 7.03 (s, 4 H, Mes), 6.97 (d, J = 7.8 Hz, 1 H, Py), 6.75

(d, J = 7.8 Hz, 1 H, Py), 4.05 (m, 4 H, $\text{NCH}_2\text{CH}_2\text{N}$), 2.91 (m, 4 H, $\text{Ru}=\text{CHCH}_2\text{CH}_2\text{Py}$), 2.61 (br s, 6

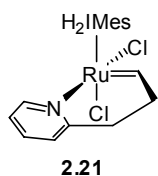
H, $\text{Mes}-\text{CH}_3$), 2.37 (s, 6 H, $\text{Mes}-\text{CH}_3$), 2.31 (br s, 6 H, $\text{Mes}-\text{CH}_3$), 2.01 (s, 3 H, $\text{Py}-\text{CH}_3$). $^{13}\text{C}\{^1\text{H}\}$

NMR (CD_2Cl_2 , 125 MHz, δ): 343.54 ($\text{Ru}=\text{CHCH}_2$), 218.21 ($\text{Ru}-\text{C}(\text{N})_2$), 160.62, 160.55, 140.45,

139.29, 138.73, 137.88, 136.65, 129.79, 128.82, 123.03, 122.13, 52.04, 51.24, 34.66, 32.20,

22.86, 21.76, 21.34, 20.37, 18.51.

Synthesis of catalyst 2.21. A flask was charged with complex **2.1** (5.0 g, 5.9 mmol). The flask



was capped, sparged with Ar for 15 min, and charged with CH_2Cl_2 (60 mL). 2-(3-

Butenyl)pyridine (1.2 g, 8.9 mmol) was then added via syringe and the reaction

mixture was heated to 40 °C for 4 d. The reaction mixture was concentrated to

dryness and the residue triturated with degassed, chilled MeOH (15 mL). The solid was collected

on a frit and washed with MeOH (2 x 10 mL) to give **2.21** (1.3 g, 2.2 mmol) as an orange-brown

solid upon drying. Yield: 37%. ^1H NMR (CD_2Cl_2 , 300 MHz, δ): 19.14 (t, J = 3.3 Hz, 1 H,

$\text{Ru}=\text{CHCH}_2$), 7.54 (d, J = 7.8 Hz, 1 H, Py), 7.49 (t, J = 5.1 Hz, 1 H, Py), 7.25 (s, 1 H, Mes), 7.06

(s, 1 H, Mes), 7.03 (d, J = 7.8 Hz, 1 H, Py), 6.90 (s, 1 H, Mes), 6.88 (s, 1 H, Mes), 6.81 (t, J = 6.6

Hz, 1 H, Py), 4.15 (m, 2 H, $\text{NCH}_2\text{CH}_2\text{N}$), 3.90 (m, 2 H, $\text{NCH}_2\text{CH}_2\text{N}$), 3.00 (m, 2 H, CH_2-Py), 2.88

(s, 3 H, $\text{Mes}-\text{CH}_3$), 2.69 (s, 3 H, $\text{Mes}-\text{CH}_3$), 2.40 (s, 3 H, $\text{Mes}-\text{CH}_3$), 2.34 (s, 3 H, $\text{Mes}-\text{CH}_3$), 1.96

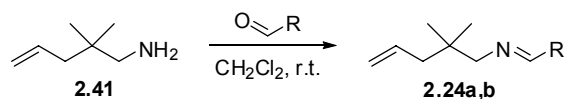
(s, 3 H, $\text{Mes}-\text{CH}_3$), 1.78 (m, 1 H, $\text{Ru}=\text{CHCH}_2$), 1.45 (s, 3 H, $\text{Mes}-\text{CH}_3$), 1.21 (m, 1 H, $\text{Ru}=\text{CH}$).

$^{13}\text{C}\{^1\text{H}\}$ NMR (CD_2Cl_2 , 125 MHz, δ): 319.04 ($\text{Ru}=\text{CHCH}_2$), 218.94 ($\text{Ru}-\text{C}(\text{N})_2$), 161.71, 154.02,

139.51, 138.94, 138.32, 137.90, 135.57, 134.97, 132.96, 130.26, 129.53, 129.34, 129.16, 128.65, 122.94, 120.00, 50.54, 49.23, 34.87, 20.52, 20.27, 19.25, 18.92, 18.39, 17.56.

Conversion of 2.20a to 2.21. In the glove box, a 0.1 M solution of **2.20a** in CD_2Cl_2 was prepared and transferred to an NMR tube, which was capped and taken out of the glove box. The NMR tube was left in an oil bath at 40 °C and the reaction was monitored by ^1H NMR spectroscopy. The composition of the mixture was the following **2.21/2.20a** = 30/70 after 24 h; 60/40 after 48 h; 70/30 after 72 h; and 78/22 after 96 h.

Conversion of 2.21 to 2.20a. In the glove box, a 0.1 M solution of **2.21** in CD_2Cl_2 was prepared and transferred to an NMR tube, which was capped and taken out of the glove box. The NMR tube was left in an oil bath at 40 °C and the reaction was monitored by ^1H NMR spectroscopy. The composition of the mixture was the following **2.21/2.20a** = 83/17 after 24 h. ^1H NMR spectroscopy also showed that the isomerization of **2.21** was accompanied with some catalyst decomposition, making it complicated to analyze the reaction mixture beyond 24 hours.

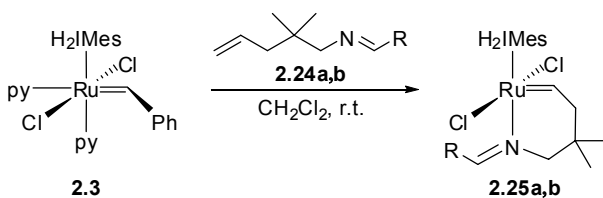


General procedure for the synthesis of imines $\text{CH}_2=\text{CHCH}_2\text{CMe}_2\text{CH}_2\text{N}=\text{CHR}$ (2,24a,b**).** The condensation of 2,2-dimethyl-4-pentenylamine (**2.41**) with various aldehydes was carried out in CH_2Cl_2 over activated 4 Å molecular sieves at r.t. for 12 h. The sieves were removed by filtration and the solution concentrated under vacuum to give the desired imines.

Imine 2.24a (R = Ph). Amine **2.41** (1.00 mL, 0.78 g, 6.9 mmol) and benzaldehyde (0.70 mL, 0.73 g, 6.9 mmol) in CH_2Cl_2 (15 mL) gave **2.24a** (0.975 g, 4.84 mmol) as a clear liquid containing approximately 8% excess benzaldehyde. Yield: 70%. ^1H NMR (CDCl_3 , 300 MHz, δ): 8.24 (s, 1 H, $\text{CH}=\text{N}$), 7.76 (m, 2 H, Ph), 7.42 (m, 3 H, Ph), 5.98–5.82 (m, 1 H, $\text{CH}_2=\text{CHCH}_2$), 5.09–5.00 (m, 2 H, $\text{CH}_2=\text{CH}$), 3.40 (s, 2 H, $\text{CMe}_2\text{CH}_2\text{N}$), 2.10 (d, $J = 7.5$ Hz, 2 H, $=\text{CHCH}_2\text{CMe}_2$), 0.98 (s, 6 H,

CMe_2). $^{13}\text{C}\{^1\text{H}\}$ NMR (CDCl_3 , 75 MHz, δ): 161.08, 136.69, 135.66, 130.57, 128.72, 128.26, 117.18, 72.27, 45.19, 35.48, 25.80. IR (CH_2Cl_2 soln, $\nu_{\text{C=N}}$, cm^{-1}): 1647.5.

Imine 2.24b (R = *t*-Bu). Amine **2.41** (0.88 mL, 0.69 g, 6.1 mmol) and trimethylacetaldehyde (0.72 mL, 0.57 g, 6.6 mmol) in CH_2Cl_2 (15 mL) gave **2.24b** (0.634 g, 3.50 mmol) as a clear liquid. Yield: 58%. ^1H NMR (CDCl_3 , 300 MHz, δ): 7.44 (t, $J = 1.5$ Hz, 1 H, CH=N), 5.91–5.76 (m, 1 H, $\text{CH}_2=\text{CHCH}_2$), 5.04–4.94 (m, 2 H, $\text{CH}_2=\text{CH}$), 3.12 (d, $J = 0.9$ Hz, 2 H, $\text{CMe}_2\text{CH}_2\text{N}$), 1.98 (dt, $J = 9.0, 1.2$ Hz, 2 H, $=\text{CHCH}_2\text{CMe}_2$), 1.06 (s, 9 H, N=CHCMe_3), 0.86 (s, 6 H, CMe_2). $^{13}\text{C}\{^1\text{H}\}$ NMR (CDCl_3 , 75 MHz, δ): 172.26, 135.74, 117.02, 71.78, 45.13, 36.38, 35.01, 27.19, 25.59. IR (CH_2Cl_2 soln, $\nu_{\text{C=N}}$, cm^{-1}): 1669.3.

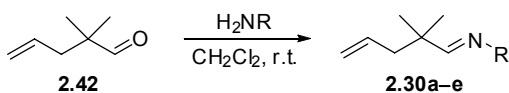


General procedure for the synthesis of catalysts 2.25a,b. In the glove box, a Schlenk flask was charged with **2.3** and CH_2Cl_2 . The corresponding imine **2.24** was then added via syringe and the reaction stirred at r.t. for 30 min. The volatiles were removed under vacuum, the residue redissolved in C_6H_6 (2 mL), and precipitated with pentane (20 mL), cooling to -5 °C. The solid was collected, washed with pentane (3 x 5 mL) and dried under vacuum to give the imine-substituted ruthenium compounds in good yields. Any modifications are described below for each reaction.

Catalyst 2.25a (R = Ph). Ru complex **2.3** (196 mg, 0.270 mmol), imine **2.24a** (68 mg, 0.34 mmol) and CH_2Cl_2 (5 mL) gave **2.25a** (151 mg, 0.135 mmol) as a light green solid. Yield: 84%. ^1H NMR (CD_2Cl_2 , 300 MHz, δ): 18.71 (t, $J = 5.7$ Hz, 1 H, Ru=CHCH_2), 8.39 (s, 1 H, CH=N), 7.31 (t, $J = 7.5$ Hz, 1 H, Bn), 7.19 (d, $J = 7.2$ Hz, 2 H, Bn), 7.06 (t, $J = 7.8$ Hz, 2 H, Bn), 7.06 (s, 4 H, Mes), 3.95 (s, 2 H, $\text{CMe}_2\text{CH}_2\text{N}$), 3.88 (s, 4 H, $\text{NCH}_2\text{CH}_2\text{N}$), 2.78 (d, $J = 5.4$ Hz, 2 H,

Ru=CHCH₂CMe₂, 2.44 (s, 12 H, Mes-CH₃), 2.41 (s, 6 H, Mes-CH₃), 0.73 (s, 6 H, CMe₂). ¹³C{¹H} NMR (CD₂Cl₂, 75 MHz, δ): 341.41 (Ru=CH), 218.02 (Ru-C(N)₂), 170.04 (Ru-N=C), 138.87, 137.29, 134.62, 130.96, 130.31, 130.11, 128.99, 77.35, 66.70, 51.91, 34.29, 26.35, 21.45, 19.41. IR (CH₂Cl₂ soln, ν_{C=N}, cm⁻¹): 1623.7. HRMS-FAB (m/z): [M]⁺ calcd for C₃₄H₄₃Cl₂N₃Ru, 665.1878; found, 665.1855.

Catalyst 2.25b (R = *t*-Bu). Ru complex **2.3** (132 mg, 0.182 mmol), imine **8b** (42 mg, 0.23 mmol) and CH₂Cl₂ (5 mL) gave **2.25b** (92 mg, 0.14 mmol) as a light green solid. Yield: 78%. ¹H NMR (CD₂Cl₂, 300 MHz, δ): 18.54 (t, *J* = 6.0 Hz, 1 H, Ru=CHCH₂), 7.45 (t, *J* = 1.5 Hz, 1 H, CH=N), 7.00 (br s, 4 H, Mes), 3.90 (br s, 4 H, NCH₂CH₂N), 3.45 (d, *J* = 1.8 Hz, 2 H, CMe₂CH₂N), 2.81 (d, *J* = 6.3 Hz, 2 H, Ru=CHCH₂CMe₂), 2.42 (br s, 12 H, Mes-CH₃), 2.35 (s, 6 H, Mes-CH₃), 0.95 (s, 9 H, N=CHCMe₃), 0.70 (s, 6 H, CMe₂). ¹³C{¹H} NMR (CD₂Cl₂, 125 MHz, δ): 343.35 (Ru=CH), 218.91 (Ru-C(N)₂), 180.80 (Ru-N=C), 138.74, 137.48, 130.02, 76.96, 66.43, 51.60, 37.02, 34.61, 26.53, 26.45, 21.36, 19.52 (br). IR (CH₂Cl₂ soln, ν_{C=N}, cm⁻¹): 1635.6. HRMS-FAB (m/z): [M]⁺ calcd for C₃₂H₄₇Cl₂N₃Ru, 645.2191; found, 645.2204.



General procedure for the synthesis of imines CH₂=CHCH₂CMe₂CH=NR (2.30a-e). The condensation of 2,2-dimethyl-4-pentenal (**2.42**) with various primary amines was carried out in CH₂Cl₂ over activated 4 Å molecular sieves at r.t. for 12 h. The sieves were removed by filtration and the solution concentrated under vacuum to give the desired imines.

Imine 2.30a (R = Ph). Aldehyde **2.42** (1.00 mL, 0.825 g, 7.35 mmol) and aniline (0.67 mL, 0.674 g, 7.35 mmol) in CH₂Cl₂ (15 mL) gave **2.30a** (1.094 g, 5.84 mmol) as a clear liquid. Yield: 79%. ¹H NMR (CDCl₃, 300 MHz, δ): 7.69 (s, 1 H, CH=N), 7.35–6.95 (m, 5 H, Ph), 5.92–5.76 (m, 1 H, CH₂=CHCH₂), 5.12–5.04 (m, 2 H, CH₂=CH), 2.29 (dt, *J* = 7.5, 1.2 Hz, 2 H, =CHCH₂CMe₂), 1.18

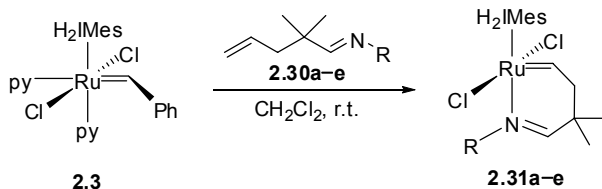
(s, 6 H, CM_{e2}). $^{13}C\{^1H\}$ NMR ($CDCl_3$, 75 MHz, δ): 172.78, 152.84, 134.58, 129.12, 125.36, 120.74, 117.98, 44.87, 39.94, 24.63. IR (CH_2Cl_2 soln, $\nu_{C=N}$, cm^{-1}): 1648.0.

Imine 2.30b (R = *i*-Pr). Aldehyde **2.42** (1.00 mL, 0.825 g, 7.35 mmol) and isopropylamine (1.25 mL, 0.867 g, 14.7 mmol) in CH_2Cl_2 (15 mL) gave **2.30b** (0.666 g, 4.34 mmol) as a clear liquid. Yield: 59%. 1H NMR ($CDCl_3$, 300 MHz, δ): 7.49 (s, 1 H, $CH=N$), 5.82–5.64 (m, 1 H, $CH_2=CHCH_2$), 5.06–4.92 (m, 2 H, $CH_2=CH$), 3.24 (sept., $J = 6.3$ Hz, 1 H, $NCHMe_2$), 2.13 (d, $J = 7.2$ Hz, 2 H, $=CHCH_2CMe_2$), 1.11 (d, $J = 6.6$ Hz, 6 H, $NCHMe_2$), 1.02 (s, 6 H, CM_{e2}). $^{13}C\{^1H\}$ NMR ($CDCl_3$, 75 MHz, δ): 168.35, 134.97, 117.41, 61.69, 44.99, 38.62, 24.92, 24.35. IR (CH_2Cl_2 soln, $\nu_{C=N}$, cm^{-1}): 1661.4.

Imine 2.30c (R = Cy). Aldehyde **2.42** (1.00 mL, 0.825 g, 7.35 mmol) and cyclohexylamine (0.88 mL, 0.762 g, 7.69 mmol) in CH_2Cl_2 (15 mL) gave **2.30c** (0.730 g, 3.77 mmol) as a clear liquid. Yield: 51%. 1H NMR ($CDCl_3$, 300 MHz, δ): 7.50 (s, 1 H, $CH=N$), 5.82–5.66 (m, 1 H, $CH_2=CHCH_2$), 5.04–4.94 (m, 2 H, $CH_2=CH$), 2.89 (tt, $J = 10.5, 4.2$ Hz, 1 H, $NCH-Cy$), 2.13 (dt, $J = 7.5$ Hz, 0.9 Hz, 2 H, $=CHCH_2CMe_2$), 1.82–1.10 (m, 10 H, Cy), 1.01 (s, 6 H, CM_{e2}). $^{13}C\{^1H\}$ NMR ($CDCl_3$, 75 MHz, δ): 168.73, 135.03, 117.37, 70.04, 45.00, 38.69, 34.60, 25.81, 25.10, 24.94. IR (CH_2Cl_2 soln, $\nu_{C=N}$, cm^{-1}): 1662.7.

Imine 2.30d (R = *t*-Bu). Aldehyde **2.42** (1.00 mL, 0.825 g, 7.35 mmol) and *tert*-butylamine (0.93 mL, 0.647 g, 8.85 mmol) in CH_2Cl_2 (15 mL) gave **2.30d** (0.555 g, 3.32 mmol) as a clear liquid. Yield: 45%. 1H NMR ($CDCl_3$, 300 MHz, δ): 7.43 (s, 1 H, $CH=N$), 5.82–5.66 (m, 1 H, $CH_2=CHCH_2$), 5.03–4.94 (m, 2 H, $CH_2=CH$), 2.14 (dt, $J = 7.5, 1.2$ Hz, 2 H, $=CHCH_2CMe_2$), 1.13 (s, 9 H, $NCMe_3$), 1.01 (s, 6 H, CM_{e2}). $^{13}C\{^1H\}$ NMR ($CDCl_3$, 75 MHz, δ): 164.63, 135.31, 117.19, 56.42, 45.09, 38.68, 29.97, 24.92. IR (CH_2Cl_2 soln, $\nu_{C=N}$, cm^{-1}): 1665.9.

Imine 2.30e (R = Ph). Aldehyde **2.42** (1.00 mL, 0.825 g, 7.35 mmol) and methylamine (2.0 M in THF, 6.00 mL, 12.0 mmol) in CH₂Cl₂ (15 mL) gave **2.30e** (0.631 g, 5.04 mmol) as a clear liquid. Yield: 69%. ¹H NMR (CDCl₃, 300 MHz, δ): 7.49 (q, *J* = 1.5 Hz, 1 H, CH=N), 5.80–5.64 (m, 1 H, CH₂=CHCH₂), 5.04–4.94 (m, 2 H, CH₂=CH), 3.23 (d, *J* = 1.5 Hz, 3 H, NMe), 2.12 (dt, *J* = 7.2, 1.2 Hz, 2 H, =CHCH₂CMe₂), 1.01 (s, 6 H, CMe₂). ¹³C{¹H} NMR (CDCl₃, 75 MHz, δ): 172.72, 134.74, 117.59, 48.08, 44.79, 39.13, 24.63. IR (CH₂Cl₂ soln, ν_{C=N}, cm⁻¹): 1670.9.



General procedure for the synthesis of catalysts 2.31a–e. In the glove box, a Schlenk flask was charged with **2.3** and CH₂Cl₂. The corresponding imine was then added via syringe and the reaction stirred at r.t. for 30 min. The volatiles were removed under vacuum, the residue redissolved in C₆H₆ (2 mL), and precipitated with pentane (20 mL), cooling to -5 °C. The solid was collected, washed with pentane (3 x 5 mL) and dried under vacuum to give the imine-substituted ruthenium compounds in good yields. Any modifications are described below for each reaction.

Catalyst 2.31a (R = Ph). Ru complex **2.3** (155 mg, 0.213 mmol), imine **2.30a** (60 mg, 0.32 mmol) and CH₂Cl₂ (5 mL) gave **2.31a** (116 mg, 0.177 mmol) as a light green solid. Yield: 83%. ¹H NMR (CD₂Cl₂, 300 MHz, δ): 18.80 (t, *J* = 5.4 Hz, 1 H, Ru=CHCH₂), 7.64 (s, 1 H, CH=N), 7.2–6.9 (m, 9 H, Ph and Mes), 4.01 (s, 4 H, NCH₂CH₂N), 3.02 (d, *J* = 5.4 Hz, 2 H, Ru=CHCH₂CMe₂), 2.5–2.3 (m, 18 H, Mes-CH₃), 1.07 (s, 6 H, CMe₂). ¹³C{¹H} NMR (CD₂Cl₂, 125 MHz, δ): 345.10 (Ru=CH), 218.03 (Ru-C(N)₂), 176.96 (Ru-N=C), 149.63, 138.81, 129.82, 129.40, 127.12, 122.48, 64.30, 51.82, 42.69, 26.89, 21.46, 19.28. IR (CH₂Cl₂ soln, ν_{C=N}, cm⁻¹): 1634.3. HRMS-FAB (*m/z*): [M]⁺ calcd for C₃₃H₄₁Cl₂N₃Ru, 651.1722; found, 651.1726. Anal. Calcd for C₃₃H₄₁Cl₂N₃Ru: C, 60.82; H, 6.34; N, 6.45. Found: C, 60.72; H, 6.38; N, 6.48.

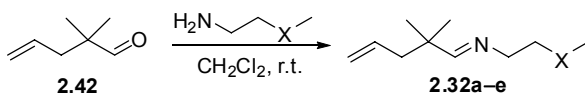
Catalyst 2.31b (R = *i*-Pr). Ru complex **2.3** (239 mg, 0.328 mmol), imine **2.30b** (76 mg, 0.49 mmol) and CH₂Cl₂ (5 mL) gave **2.31b** (162 mg, 0.262 mmol) as a light green solid. Yield: 80%. ¹H NMR (CD₂Cl₂, 300 MHz, δ): 18.58 (t, *J* = 5.4 Hz, 1 H, Ru=CHCH₂), 7.41 (d, *J* = 1.5 Hz, 1 H, CH=N), 6.99 (s, 4 H, Mes), 4.02 (s, 4 H, NCH₂CH₂N), 3.32 (sept.d, *J* = 6.6, 1.5 Hz, 1H, NCHMe₂), 2.96 (d, *J* = 5.4 Hz, 2 H, Ru=CHCH₂CMe₂), 2.42 (br s, 12 H, Mes-CH₃), 2.34 (s, 6 H, Mes-CH₃), 0.92 (s, 6 H, CMe₂), 0.90 (d, *J* = 6.9 Hz, 6 H, NCHMe₂). ¹³C{¹H} NMR (CD₂Cl₂, 125 MHz, δ): 345.17 (Ru=CH), 219.54 (Ru-C(N)₂), 173.68 (Ru-N=C), 138.91, 129.74, 64.21, 60.78, 51.60, 42.51, 26.96, 22.47, 21.36, 19.36 (br). IR (CH₂Cl₂ soln, ν_{C=N}, cm⁻¹): 1642.6. HRMS-FAB (*m/z*): [M]⁺ calcd for C₃₀H₄₃Cl₂N₃Ru, 617.1878; found, 617.1853.

Catalyst 2.31c (R = Cy). Ru complex **2.3** (192 mg, 0.263 mmol), imine **2.30c** (74 mg, 0.38 mmol) and CH₂Cl₂ (5 mL) gave **2.31c** (146 mg, 0.222 mmol) as a light green solid. Yield: 84%. ¹H NMR (CD₂Cl₂, 300 MHz, δ): 18.56 (t, *J* = 5.4 Hz, 1 H, Ru=CHCH₂), 7.41 (d, *J* = 0.9 Hz, 1 H, CH=N), 7.00 (br s, 4 H, Mes), 4.00 (br s, 4 H, NCH₂CH₂N), 2.96 (d, *J* = 5.7 Hz, 2 H, Ru=CHCH₂CMe₂), 2.7-2.2 (br m, 12 H, Mes-CH₃), 2.34 (s, 6 H, Mes-CH₃), 1.7-0.8 (m, 11 H, Cy), 0.91 (s, 6 H, CMe₂). ¹³C{¹H} NMR (CD₂Cl₂, 125 MHz, δ): 345.00 (Ru=CH), 219.49 (Ru-C(N)₂), 173.76 (Ru-N=C), 138.76, 129.76, 69.99, 64.07, 51.63, 42.23, 33.47, 26.90, 26.10, 25.49, 21.39, 20.00 (br), 18.78 (br). IR (CH₂Cl₂ soln, ν_{C=N}, cm⁻¹): 1641.1. HRMS-FAB (*m/z*): [M]⁺ calcd for C₃₃H₄₇Cl₂N₃Ru, 657.2191; found, 657.2163.

Catalyst 2.31d (R = *t*-Bu). Ru complex **2.3** (188 mg, 0.258 mmol), imine **2.30d** (56 mg, 0.34 mmol) and CH₂Cl₂ (5 mL) gave **2.31d** (91 mg, 0.143 mmol) as a light green solid. Yield: 56%. ¹H NMR (CD₂Cl₂, 300 MHz, δ): 18.37 (t, *J* = 5.7 Hz, 1 H, Ru=CHCH₂), 7.43 (s, 1 H, CH=N), 7.04-6.94 (m, 4 H, Mes), 4.10-3.96 (m, 4 H, NCH₂CH₂N), 3.08 (d, *J* = 5.4 Hz, 2 H, Ru=CHCH₂CMe₂), 2.59 (br s, 6 H, Mes-CH₃), 2.34 (s, 6 H, Mes-CH₃), 2.26 (br s, 6 H, Mes-CH₃), 1.01 (s, 9 H, NCM₃), 0.92 (s, 6 H, CMe₂). ¹³C{¹H} NMR (CD₂Cl₂, 125 MHz, δ): 345.22 (Ru=CH), 219.82 (Ru-C(N)₂), 172.97 (Ru-N=C), 139.83, 139.13, 138.55, 137.92, 136.09, 129.83, 129.74,

64.05, 63.66, 51.75, 51.27, 43.02, 28.89, 26.77, 21.37, 20.21, 18.58. IR (CH₂Cl₂ soln, $\nu_{C=N}$, cm⁻¹): 1638.6. HRMS-FAB (m/z): [M]⁺ calcd for C₃₁H₄₅Cl₂N₃Ru, 631.2035; found, 631.2031.

Catalyst 2.31e (R = Me). Ru complex **2.3** (143 mg, 0.196 mmol), imine **2.30e** (30 mg, 0.24 mmol) and CH₂Cl₂ (5 mL) gave **2.31e** (93 mg, 0.16 mmol) as a green-brown solid. Yield: 84%. ¹H NMR (CD₂Cl₂, 300 MHz, δ): 18.80 (t, J = 5.1 Hz, 1 H, Ru=CHCH₂), 7.42 (m, 1 H, CH=N), 7.00 (br s, 4 H, Mes), 4.05 (s, 4 H, NCH₂CH₂N), 2.73 (d, J = 1.2 Hz, 1H, NMe), 2.69 (d, J = 5.1 Hz, 2 H, Ru=CHCH₂CMe₂), 2.41 (s, 12 H, Mes-CH₃), 2.34 (s, 6 H, Mes-CH₃), 0.93 (s, 6 H, CMe₂). ¹³C{¹H} NMR (CD₂Cl₂, 125 MHz, δ): 342.54 (Ru=CH), 218.93 (Ru-C(N)₂), 175.29 (Ru-N=C), 139.04, 138.87, 136.52, 129.61, 64.46, 51.85, 46.76, 41.83, 26.88, 21.37, 19.56. IR (CH₂Cl₂ soln, $\nu_{C=N}$, cm⁻¹): 1635.4. HRMS-FAB (m/z): [M]⁺ calcd for C₂₈H₃₉Cl₂N₃Ru, 589.1565; found, 589.1560.



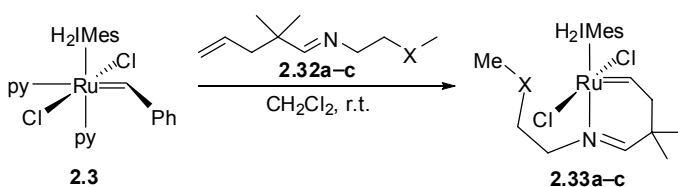
General procedure for the synthesis of imines CH₂=CHCH₂CMe₂CH=NCH₂CH₂XMe (2.32a-c). The condensation of 2,2-dimethyl-4-pentenal (**2.42**) with various primary amines was carried out in CH₂Cl₂ over activated 4Å molecular sieves at r.t. for 12 h. The sieves were removed by filtration and the solution concentrated under vacuum to give the desired imines.

Imine 2.32a (X = CH₂). Aldehyde **2.42** (1.00 mL, 0.825 g, 7.35 mmol) and *n*-butylamine (1.09 mL, 0.806 g, 11.0 mmol) in CH₂Cl₂ (15 mL) gave **2.32a** (0.705 g, 4.22 mmol) as a clear liquid. Yield: 57%. ¹H NMR (CDCl₃, 300 MHz, δ): 7.47 (t, J = 1.2 Hz, 1 H, CH=N), 5.82–5.66 (m, 1 H, CH₂=CHCH₂), 5.06–4.94 (m, 2 H, CH₂=CH), 3.36 (td, J = 7.2, 1.2 Hz, 2 H, CH=NCH₂CH₂), 2.14 (d, J = 7.5 Hz, 2 H, =CHCH₂CMe₂), 1.54 (quint., J = 7.5 Hz, 2 H, NCH₂CH₂CH₂), 1.27 (sext., J = 7.8 Hz, CH₂CH₂Me), 1.03 (s, 6 H, CMe₂), 0.89 (t, J = 7.2 Hz, 3 H, Bu-Me). ¹³C{¹H} NMR (CDCl₃,

75 MHz, δ): 171.12, 134.87, 117.51, 61.33, 44.92, 39.02, 33.15, 24.82, 20.40, 14.04. IR (CH_2Cl_2 soln, $\nu_{\text{C=N}}$, cm^{-1}): 1665.6.

Imine 2.32b (X = O). Aldehyde **2.42** (1.00 mL, 0.825 g, 7.35 mmol) and 2-methoxyethylamine (0.77 mL, 0.662 g, 8.82 mmol) in CH_2Cl_2 (15 mL) gave **2.32b** (0.946 g, 5.59 mmol) as a clear liquid. Yield: 76%. ^1H NMR (CDCl_3 , 300 MHz, δ): 7.53 (s, 1 H, CH=N), 5.83–5.67 (m, 1 H, $\text{CH}_2=\text{CHCH}_2$), 5.06–4.97 (m, 2 H, $\text{CH}_2=\text{CH}$), 3.55 (s, 4 H, $\text{CH=NCH}_2\text{CH}_2$), 3.34 (s, 3 H, OMe), 2.15 (d, $J = 7.2$ Hz, 2 H, $=\text{CHCH}_2\text{CMe}_2$), 1.05 (s, 6 H, CMe_2). $^{13}\text{C}\{^1\text{H}\}$ NMR (CDCl_3 , 75 MHz, δ): 173.29, 134.80, 117.50, 72.29, 60.98, 58.98, 44.84, 39.19. IR (CH_2Cl_2 soln, $\nu_{\text{C=N}}$, cm^{-1}): 1666.6.

Imine 2.32c (X = S). Aldehyde **2.42** (1.00 mL, 0.825 g, 7.35 mmol) and 2-thiomethylethylamine (0.69 mL, 0.67 g, 7.37 mmol) in CH_2Cl_2 (15 mL) gave **2.32c** (1.150 g, 6.20 mmol) as a pale yellow liquid. Yield: 84%. ^1H NMR (CDCl_3 , 300 MHz, δ): 7.53 (t, $J = 1.2$ Hz, 1 H, CH=N), 5.84–5.70 (m, 1 H, $\text{CH}_2=\text{CHCH}_2$), 5.06–4.98 (m, 2 H, $\text{CH}_2=\text{CH}$), 3.58 (td, $J = 7.2, 1.2$ Hz, 2 H, $\text{CH=NCH}_2\text{CH}_2$), 2.71 (t, $J = 7.2$ Hz, 2 H, $\text{NCH}_2\text{CH}_2\text{SMe}$), 2.16 (td, $J = 7.5, 1.2$ Hz, 2 H, $=\text{CHCH}_2\text{CMe}_2$), 2.12 (s, 3 H, CH_2SMe), 1.05 (s, 6 H, CMe_2). $^{13}\text{C}\{^1\text{H}\}$ NMR (CDCl_3 , 75 MHz, δ): 172.93, 134.71, 117.66, 60.97, 44.81, 39.23, 35.23, 24.69, 16.09. IR (CH_2Cl_2 soln, $\nu_{\text{C=N}}$, cm^{-1}): 1664.6.



General procedure for the synthesis of catalysts 2.33a–c. In the glove box, a Schlenk flask was charged with **2.3** and CH_2Cl_2 . The corresponding imine **2.32** was then added via syringe and the reaction stirred at r.t. for 30 min. The volatiles were removed under vacuum, the residue redissolved in C_6H_6 (2 mL), and precipitated with pentane (20 mL), cooling to -5 °C. The solid was collected, washed with pentane (3 x 5 mL) and dried under vacuum to give the imine-

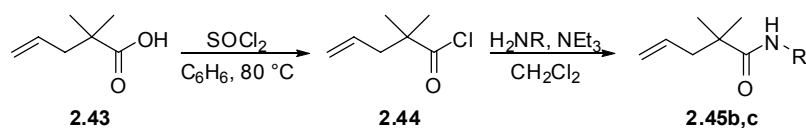
substituted ruthenium compounds in good yields. Any modifications are described below for each reaction.

Catalyst 2.33a (X = CH₂). Ru complex **2.3** (140 mg, 0.192 mmol), imine **2.32a** (48 mg, 0.22 mmol) and CH₂Cl₂ (5 mL) gave **2.33a** (85 mg, 0.14 mmol) as a light green solid. Yield: 70%. ¹H NMR (CD₂Cl₂, 300 MHz, δ): 18.71 (t, *J* = 5.4 Hz, 1 H, Ru=CHCH₂), 7.38 (t, *J* = 1.2 Hz, 1 H, CH=N), 7.00 (br s, 4 H, Mes), 4.03 (s, 4 H, NCH₂CH₂N), 3.03 (td, *J* = 7.8, 1.2 Hz, 2 H, CH=NCH₂CH₂), 2.84 (d, *J* = 5.4 Hz, 2 H, Ru=CHCH₂CMe₂), 2.42 (br s, 12 H, Mes-CH₃), 2.34 (s, 6 H, Mes-CH₃), 1.19 (m, 2 H, NCH₂CH₂CH₂), 1.04 (sext., *J* = 7.8 Hz, 2 H, CH₂CH₂Me), 0.93 (s, 6 H, CMe₂), 0.77 (t, *J* = 7.5 Hz, 3 H, Bu-Me). ¹³C{¹H} NMR (CD₂Cl₂, 125 MHz, δ): 344.20 (Ru=CH), 219.23 (Ru-C(N)₂), 174.25 (Ru-N=C), 138.84, 129.74, 64.54, 61.70, 51.72 (br), 42.00, 31.14, 27.04, 21.40, 20.89, 19.58 (br), 13.61. IR (CH₂Cl₂ soln, ν_{C=N}, cm⁻¹): 1634.9. HRMS-FAB (*m/z*): [M]⁺ calcd for C₃₁H₄₅Cl₂N₃Ru, 631.2035; found, 631.2042.

Catalyst 2.33b (X = O). Ru complex **2.3** (160 mg, 0.220 mmol), imine **2.32b** (47 mg, 0.28 mmol) and CH₂Cl₂ (5 mL) gave **2.33b** (116 mg, 0.182 mmol) as a light green solid. Yield: 83%. ¹H NMR (CD₂Cl₂, 300 MHz, δ): 18.64 (t, *J* = 5.7 Hz, 1 H, Ru=CHCH₂), 7.47 (t, *J* = 1.5 Hz, 1 H, CH=N), 7.00 (s, 4 H, Mes), 3.93 (s, 4 H, NCH₂CH₂N), 3.53 (t, *J* = 5.4 Hz, 2 H, NCH₂CH₂OMe), 3.14 (td, *J* = 5.8, 1.5 Hz, 2 H, CH=NCH₂CH₂), 2.92 (d, *J* = 5.4 Hz, 2 H, Ru=CHCH₂CMe₂), 2.83 (s, 3 H, OMe), 2.44 (s, 12 H, Mes-CH₃), 2.35 (s, 6 H, Mes-CH₃), 0.95 (s, 6 H, CMe₂). ¹³C{¹H} NMR (CD₂Cl₂, 75 MHz, δ): 341.29 (Ru=CH), 218.88 (Ru-C(N)₂), 176.24 (Ru-N=C), 139.03, 138.64, 137.40, 129.73, 70.46, 63.31, 59.33, 58.61, 51.95, 40.89, 26.96, 21.35, 19.49. IR (CH₂Cl₂ soln, ν_{C=N}, cm⁻¹): 1645.8. HRMS-FAB (*m/z*): [M]⁺ calcd for C₃₀H₄₃Cl₂N₃RuO, 633.1827; found, 633.1845.

Catalyst 2.33c (X = S). Ru complex **2.3** (149 mg, 0.205 mmol), imine **2.32c** (47 mg, 0.25 mmol) and CH₂Cl₂ (5 mL) gave **2.33c** (110 mg, 0.169 mmol) as a light green solid. Yield: 83%. ¹H NMR

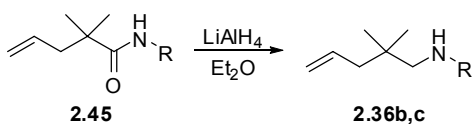
(CD₂Cl₂, 300 MHz, δ): 18.45 (t, $J = 7.5$ Hz, 1 H, Ru=CHCH₂), 7.47 (s, 1 H, CH=N), 7.01 (s, 4 H, Mes), 3.79 (s, 4 H, NCH₂CH₂N), 3.13 (m, 4 H, NCH₂CH₂ and Ru=CHCH₂CMe₂), 2.5–2.4 (m, 2 H, NCH₂CH₂SMe), 2.42 (s, 12 H, Mes-CH₃), 2.37 (s, 6 H, Mes-CH₃), 1.43 (s, 3 H, CH₂SMe), 0.95 (s, 6 H, CMe₂). ¹³C{¹H} NMR (CD₂Cl₂, 75 MHz, δ): 342.16 (Ru=CHCH₂), 219.28 (Ru-C(N)₂), 175.04 (Ru-N=C), 139.14, 138.90, 138.44, 129.96, 61.52, 60.61, 51.89, 38.58, 35.32, 27.04, 21.40, 19.40, 14.44. IR (CH₂Cl₂ soln, $\nu_{C=N}$, cm⁻¹): 1641.3. HRMS-FAB (m/z): [M]⁺ calcd for C₃₀H₄₃Cl₂N₃RuS, 649.1599; found, 649.1626.



General procedure for the synthesis of amides 2.45b,c. 2,2-dimethyl-4-pentenoic acid (**2.43**) and SOCl₂ were dissolved in C₆H₆ (10 mL) and heated for 16 h at 80 °C, after which time the solvent was removed under reduced pressure. The resulting acid chloride (**2.44**) was dissolved in CH₂Cl₂ (30 mL) with NEt₃ and the appropriate amine. The mixture was stirred 16 h at r.t. before quenching with NaHCO₃. The layers were separated and the aqueous fraction extracted with CH₂Cl₂. The combined organics were washed with NaHCO₃ and brine and then dried over MgSO₄. The solvent was removed under reduced pressure to give the amide product **2.45**.

Amide 2.45b (R = *i*-Pr). Acid **2.43** (1.16 g, 9.08 mmol) and SOCl₂ (1.01 mL, 1.65 g, 14.0 mmol) in C₆H₆ followed by isopropylamine (1.19 mL, 0.826 g, 13.97 mmol) and NEt₃ (1.32 mL, 0.958 g, 9.47 mmol) in CH₂Cl₂ gave amide **2.45b** (1.14 g, 6.80 mmol) as a white solid. Yield: 75%. ¹H NMR (CDCl₃, 300 MHz, δ): 5.78–5.62 (m, 1 H, CH₂CHCH₂), 5.40 (br s, 1 H, NH*i*-Pr), 5.08–4.98 (m, 2 H, CH₂=CH), 4.05 (m, 1 H, NCHMe₂), 2.22 (dt, $J = 7.2, 1.2$ Hz, 2 H, =CHCH₂CMe₂), 1.12 (s, 6 H, CMe₂), 1.10 (d, $J = 6.6$ Hz, 1 H, CHMe₂). ¹³C{¹H} NMR (CDCl₃, 75 MHz, δ): 176.36, 134.65, 118.00, 45.98, 45.44, 41.35, 25.26, 22.95.

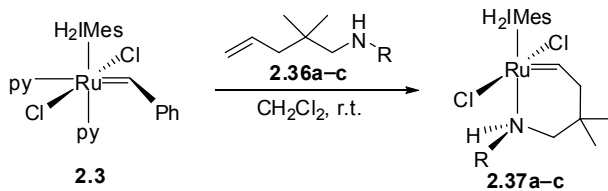
Amide 2.45c (R = Me). Acid **2.43** (1.15 g, 8.94 mmol) and SOCl_2 (0.99 mL, 1.61 g, 13.6 mmol) in C_6H_6 followed by methylamine (2.0 M in THF, 8.0 mL, 14.0 mmol) and NEt_3 (1.3 mL, 0.95 g, 9.32 mmol) in CH_2Cl_2 gave amide **2.45c** (1.10 g, 7.86 mmol) as a white solid. Yield: 88%. ^1H NMR (CDCl_3 , 300 MHz, δ): 5.8 (br s, 1 H, NHMe), 5.76–5.61 (m, 1 H, CH_2CHCH_2), 5.05–4.96 (m, 2 H, $\text{CH}_2=\text{CH}$), 2.75 (d, $J = 4.8$ Hz, 3 H, NHCH_3), 2.23 (dt, $J = 7.5, 1.2$ Hz, 2 H, $=\text{CHCH}_2\text{CMe}_2$), 1.12 (s, 6 H, CMe_2). $^{13}\text{C}\{^1\text{H}\}$ NMR (CDCl_3 , 75 MHz, δ): 178.06, 134.66, 117.93, 45.32, 42.09, 26.55, 25.21.



General procedure for the synthesis of amines 2.36b,c. To a flame-dried flask were added amide **2.45**, LiAlH_4 , and Et_2O (20 mL) stirring the resulting mixture overnight. The reaction was quenched with H_2O and dried with MgSO_4 . The liquid was filtered through celite and concentrated to give the amine product **2.36**.

Amine 2.36b (R = *i*-Pr). Amide **2.45b** (1.11 g, 6.62 mmol) and LiAlH_4 (0.30 g, 7.97 mmol) gave amine **2.36b** (0.83 g, 5.32 mmol) as a clear liquid. Yield: 80%. ^1H NMR (CDCl_3 , 300 MHz, δ): 5.89–5.73 (m, 1 H, CH_2CHCH_2), 5.05–4.96 (m, 2 H, $\text{CH}_2=\text{CH}$), 2.69 (sept., $J = 6.0$ Hz, 1 H, NHCHMe_2), 2.33 (s, 2 H, $\text{CMe}_2\text{CH}_2\text{NH}$), 1.99 (dt, $J = 7.5, 1.2$ Hz, 2 H, $=\text{CHCH}_2\text{CMe}_2$), 1.02 (d, $J = 6.0$ Hz, 6 H, NHCHMe_2), 0.87 (s, 6 H, CMe_2). $^{13}\text{C}\{^1\text{H}\}$ NMR (CDCl_3 , 75 MHz, δ): 135.88, 116.87, 58.20, 49.74, 44.89, 34.27, 25.74, 23.35.

Amine 2.36c (R = Me). Amide **2.45c** (0.89 g, 6.38 mmol) and LiAlH_4 (0.95 g, 25.0 mmol) gave amine **2.36c** (0.36 g, 2.80 mmol) as a clear liquid. Yield: 44%. ^1H NMR (CDCl_3 , 300 MHz, δ): 5.87–5.72 (m, 1 H, CH_2CHCH_2), 5.04–4.94 (m, 2 H, $\text{CH}_2=\text{CH}$), 2.41 (s, 3 H, NHCH_3), 2.31 (s, 2 H, $\text{CMe}_2\text{CH}_2\text{NH}$), 1.98 (dt, $J = 7.2, 1.2$ Hz, 2 H, $=\text{CHCH}_2\text{CMe}_2$), 0.87 (s, 6 H, CMe_2). $^{13}\text{C}\{^1\text{H}\}$ NMR (CDCl_3 , 75 MHz, δ): 135.62, 116.99, 63.34, 45.03, 37.81, 34.36, 25.70.



General procedure for the synthesis of catalysts 2.37a–c. In the glove box, a Schlenk flask was charged with **2.3** and CH_2Cl_2 . The corresponding amine **2.36** was then added via syringe and the reaction stirred at r.t. for 15 min. The volatiles were removed under vacuum and the residue was purified by column chromatography (Et_2O /pentane) and dried under vacuum to give the catalysts **2.37**.

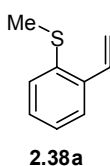
Catalyst 2.37a (R = Ph). Ru complex **2.3** (141 mg, 0.19 mmol), amine **2.36a** (46 mg, 0.25 mmol) and CH_2Cl_2 (5 mL) gave a residue that was chromatographed (Et_2O /pentane, 5% then 50%) to give **2.37a** (94 mg, 0.14 mmol) as a green solid. Yield: 75%. ^1H NMR (CD_2Cl_2 , 300 MHz, δ): 18.98 (t, $J = 5.4$ Hz, 1 H, $\text{Ru}=\text{CHCH}_2$), 7.12–6.97 (m, 5 H, NPh), 6.85 (br s, 2 H, Mes), 7.0–6.6 (br s, 2 H, Mes), 4.25 (t, $J = 12.3$ Hz, 1 H, CH_2NHP), 3.98 (br s, 4 H, $\text{NCH}_2\text{CH}_2\text{N}$), 3.48–3.32 (m, 2 H, $\text{CMe}_2\text{CH}_2\text{NHP}$), 2.9–1.7 (br m, 12 H, Mes-CH_3), 2.30 (br s, 6 H, Mes-CH_3), 2.20 (dd, $J = 12.3, 5.1$ Hz, 2 H, $\text{Ru}=\text{CHCH}_2\text{CMe}_2$), 1.07 (s, 3 H, CMe_2), 0.56 (s, 3 H, CMe_2). $^{13}\text{C}\{^1\text{H}\}$ NMR (CD_2Cl_2 , 75 MHz, δ): 346.42 ($\text{Ru}=\text{CH}$), 218.83 ($\text{Ru}-\text{C}(\text{N})_2$), 144.63, 138.59, 129.73, 129.69, 129.01, 124.44, 120.78, 67.33, 58.80, 51.74 (br), 35.13, 29.83, 23.95, 21.44, 19.45 (br). HRMS–FAB (m/z): $[\text{M}]^+$ calcd for $\text{C}_{33}\text{H}_{43}\text{Cl}_2\text{N}_3\text{Ru}$, 653.1878; found, 653.1865.

Catalyst 2.37b (R = *i*-Pr). Ru complex **2.3** (154 mg, 0.21 mmol), amine **2.36b** (41 mg, 0.26 mmol) and CH_2Cl_2 (5 mL) gave a residue that was chromatographed (Et_2O /pentane, 5% then 20%) to give **2.37b** (78 mg, 0.14 mmol) as a green solid. Yield: 60%. ^1H NMR (CD_2Cl_2 , 300 MHz, δ): 18.46 (t, $J = 5.4$ Hz, 1 H, $\text{Ru}=\text{CHCH}_2$), 7.06–6.80 (m, 4 H, Mes), 4.2–3.7 (m, 4 H, $\text{NCH}_2\text{CH}_2\text{N}$), 3.14 (m, 2 H, $\text{CMe}_2\text{CH}_2\text{NH}$ & NCHMe_2), 3.06 (dd, $J = 11.1, 5.4$ Hz, 1 H, $\text{Ru}=\text{CHCH}_2\text{CMe}_2$), 2.78 (br s, 3 H, Mes-CH_3), 2.58 (br s, 3 H, Mes-CH_3), 2.46 (dd, $J = 11.1, 5.4$ Hz, 1 H, $\text{Ru}=\text{CHCH}_2\text{CMe}_2$), 2.32 (br s, 9 H, Mes-CH_3), 2.22 (dd, $J = 11.4, 3.0$ Hz, 1 H,

$\text{CMe}_2\text{CH}_2\text{NH}$), 1.85 (br s, 3 H, Mes- CH_3), 1.00 (m, 1 H, CH_2NH), 0.93 (s, 3 H, CMe_2), 0.89 (d, $J = 6.0$ Hz, 3 H, NHCHMe_2), 0.45 (d, $J = 6.0$ Hz, 3 H, NHCHMe_2), 0.33 (s, 3 H, CMe_2). $^{13}\text{C}\{^1\text{H}\}$ NMR (CD_2Cl_2 , 75 MHz, δ): 342.93 (Ru=CH), 220.98 (Ru-C(N) $_2$), 140.19, 139.93, 139.28, 138.51, 138.04, 137.60, 135.94, 129.72, 66.39, 58.70, 51.67, 51.15, 35.93, 29.83, 23.50, 22.08, 21.98, 21.34, 20.33, 20.01, 18.90, 18.02. HRMS-FAB (m/z): $[\text{M}]^+$ calcd for $\text{C}_{30}\text{H}_{45}\text{Cl}_2\text{N}_3\text{Ru}$, 619.2035; found, 619.2037.

Catalyst 2.37c (R = Me). Ru complex **2.3** (154 mg, 0.21 mmol), amine **2.36c** (80 mg, 0.11 mmol) and CH_2Cl_2 (5 mL) gave a residue that was chromatographed (Et_2O /pentane, 10% then 50%) to give **2.37c** (28 mg, 0.14 mmol) as a green solid. Yield: 44%. ^1H NMR (CD_2Cl_2 , 300 MHz, δ): 18.83 (t, $J = 4.8$ Hz, 1 H, Ru=CH CH_2), 7.00 (br s, 2 H, Mes), 6.95 (br s, 2 H, Mes), 4.05 (br s, 4 H, NCH $_2$ CH $_2$ N), 3.43 (m, 1 H, $\text{CMe}_2\text{CH}_2\text{NH}$), 3.23 (m 1 H, Ru=CHCH $_2$ CMe $_2$), 2.8–1.8 (br s, 6 H, Mes- CH_3), 2.45 (br s, 6 H, Mes- CH_3), 2.32 (s, 6 H, Mes- CH_3), 1.98–1.92 (m, 2 H, Ru=CHCH $_2$ CMe $_2$ & $\text{CMe}_2\text{CH}_2\text{NH}$), 1.90 (d, $J = 6.0$ Hz, 3 H, NHCH_3), 1.38 (m, 1 H, CH_2NH), 0.93 (s, 3 H, CMe_2), 0.38 (s, 3 H, CMe_2). $^{13}\text{C}\{^1\text{H}\}$ NMR (CD_2Cl_2 , 75 MHz, δ): 344.08 (Ru=CH), 220.50 (Ru-C(N) $_2$), 138.83, 129.62, 129.54, 67.08, 61.94, 51.59, 36.09, 35.81, 29.54, 24.20, 21.36, 19.60. HRMS-FAB (m/z): $[\text{M}]^+$ calcd for $\text{C}_{28}\text{H}_{41}\text{Cl}_2\text{N}_3\text{Ru}$, 591.1722; found, 591.1726.

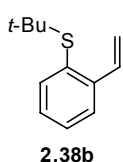
Synthesis of 2-(methylthio)styrene (2.38a). Methyltriphenylphosphonium bromide (5.54 g, 15.5



mmol) was suspended in THF (30 mL) and cooled to 0 °C. *n*-BuLi (1.6 M in hexane, 7.5 mL, 12.0 mmol) was added to give a red-orange solution that was stirred for 1 h. 2-(methylthio)benzaldehyde (1.18 g, 7.75 mmol) was added and the solution immediately changed color to a milky white suspension that was stirred for 1 h, warming to r.t. The reaction was quenched with acetone (2 mL) and poured into pentane (300 mL). The mixture was filtered through celite and concentrated to a yellow oil that was purified by column chromatography (1% EtOAc/hexanes, $R_f = 0.25$) to give **2.38a** (0.94 g, 6.2 mmol) as a clear liquid. Yield: 80%. ^1H NMR (CDCl_3 , 300 MHz, δ): 7.49 (m, 1 H, Aryl H), 7.26 (m, 2 H, Aryl H),

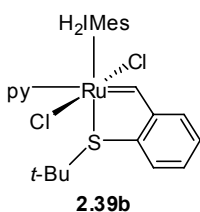
7.20–7.16 (m, 2 H, Aryl H, ArCH=CH₂), 5.69 (dd, *J* = 17.4, 1.2 Hz, 1 H, CH=CH₂), 5.35 (dd, *J* = 11.1, 1.2 Hz, 1 H, CH=CH₂), 2.46 (s, 3 H, SCH₃). ¹³C{¹H} NMR (CD₂Cl₂): δ 137.24, 136.84, 134.42, 128.42, 127.00, 126.14, 125.72, 116.13, 16.54.

Synthesis of 2-(*tert*-butylthio)styrene (2.38b). Methyltriphenylphosphonium bromide (4.68 g,



13.1 mmol) was suspended in THF (40 mL) and cooled to 0 °C. *n*-BuLi (1.6 M in hexane, 6.8 mL, 10.9 mmol) was added to give a red-orange solution that was stirred for 1 h. 2-(*t*-butylthio)benzaldehyde (1.69 g, 8.69 mmol) was added and the solution immediately changed color to a milky white suspension that was stirred for 30 min warming to r.t. The reaction was quenched with acetone (2 mL) and poured into pentane (250 mL). The mixture was filtered through celite and concentrated to a yellow oil that was purified by column chromatography (1% EtOAc/hexanes, R_f = 0.30) to give **2.38b** (1.33 g, 7.0 mmol) as a clear liquid. Yield: 80%. ¹H NMR (CDCl₃, 300 MHz, δ): 7.66 (dd, *J* = 7.8, 1.5 Hz, 1 H, Aryl H), 7.57 (dd, *J* = 18.0, 11.1 Hz, 1 H, ArCH=CH₂), 7.56 (dd, *J* = 7.5, 1.5 Hz, 1 H, Aryl H), 7.35 (m, 1 H, Aryl H), 7.23 (td, *J* = 7.5, 1.5 Hz, 1 H, Aryl H), 5.70 (dd, *J* = 18.0, 1.2 Hz, 1 H, CH=CH₂), 5.30 (dd, *J* = 11.1, 1.2 Hz, 1 H, CH=CH₂), 1.28 (s, 9 H, SCMe₃). ¹³C{¹H} NMR (CD₂Cl₂): δ 143.33, 139.74, 136.81, 131.82, 129.51, 127.79, 125.81, 115.12, 47.92, 31.39.

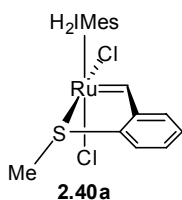
Synthesis of catalyst 2.39b. In the glove box, a flask was charged with **2.3** (159 mg, 0.22



mmol) and C₆H₆ (5 mL). Styrene **2.38b** (85 mg, 0.44 mmol) was then added via syringe and the reaction allowed to stir for 1 h before the volatiles were removed under vacuum. The residue was redissolved in C₆H₆ (2 mL) and precipitated with pentane (20 mL), cooling to -5 °C. The solid was collected, washed with pentane (3 x 5 mL) and dried under vacuum to give **2.39b** (148 mg, 0.20 mmol) as a light green solid. Yield: 92%. ¹H NMR (CD₂Cl₂): δ 17.49 (s, 1 H, Ru=CH), 8.77 (d, *J* = 3.9 Hz, 1 H, Py), 7.62 (m, 1 H, Py), 7.47 (m, 2 H, Py/Aryl H), 7.18 (m, 3 H, Py/Aryl H), 6.97 (s, 4 H, Mes), 6.70 (d, *J* = 7.5 Hz, 1 H, Aryl H), 4.04 (s, 4 H, NCH₂CH₂N), 2.45 (s, 12 H, Mes-CH₃), 2.36 (s, 6 H, Mes-CH₃), 0.90 (s, 9 H, SCMe₃). ¹³C{¹H} NMR (CD₂Cl₂): δ 313.32 (Ru=CH), 208.46 (Ru-C(N)₂),

164.48, 151.41, 138.53, 135.34, 133.02, 132.81, 129.88, 127.97, 123.61, 120.65, 52.52, 50.44, 29.01, 21.30, 19.49.

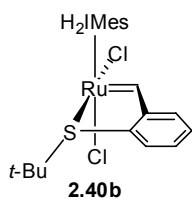
Synthesis of catalyst 2.40a. In the glove box, a flask was charged with **2.3** (145 mg, 0.20



mmol) and CH_2Cl_2 (5 mL). Styrene **2.38a** (46 mg, 0.30 mmol) was then added via syringe and the reaction allowed to stir for 6 h before the volatiles were removed under vacuum. The residue was redissolved in CH_2Cl_2 (2 mL) and precipitated with pentane (20 mL), cooling to $-5\text{ }^\circ\text{C}$. The solid was collected,

washed with pentane (3 x 5 mL) and dried under vacuum to give **2.40a** (109 mg, 0.18 mmol) as a blue-green solid. Yield: 89%. ^1H NMR (CD_2Cl_2): δ 17.00 (s, 1 H, Ru=CH), 7.54–7.42 (m, 2 H, Aryl H), 7.17 (m, 1 H, Aryl H), 7.12 (s, 1 H, Mes), 7.05 (s, 1 H, Mes), 6.93 (s, 1 H, Mes), 6.81 (d, $J = 7.5$ Hz, 1 H, Aryl H), 6.04 (s, 1 H, Mes), 4.19–3.79 (m, 4 H, $\text{NCH}_2\text{CH}_2\text{N}$), 2.65 (s, 3 H, Mes- CH_3), 2.50 (s, 3 H, Mes- CH_3), 2.48 (s, 3 H, Mes- CH_3), 2.41 (s, 3 H, Mes- CH_3), 2.38 (s, 3 H, Mes- CH_3), 2.17 (s, 3 H, Mes- CH_3), 1.58 (s, 3 H, SCH_3). $^{13}\text{C}\{^1\text{H}\}$ NMR (CD_2Cl_2): δ 285.35 (Ru=CH), 214.53 (Ru-C(N) $_2$), 155.27, 140.54, 140.38, 140.35, 138.81, 137.99, 137.06, 135.84, 135.82, 131.83, 130.92, 129.82, 129.79, 129.78, 129.57, 129.43, 128.82, 123.77, 51.79, 51.68, 21.46, 21.16, 20.42, 19.12, 18.85, 18.14, 17.54. HRMS-FAB (m/z): $[\text{M}]^+$ calcd for $\text{C}_{29}\text{H}_{34}\text{Cl}_2\text{N}_2\text{SRu}$, 614.0864; found, 614.0873.

Synthesis of catalyst 2.40b. A sample of catalyst **2.39b** (97 mg, 0.15 mmol) was dissolved in



CH_2Cl_2 (1 mL) and left at r.t. for 4 d. The sample was added to a vial and precipitated with pentane (20 mL), cooling to $-5\text{ }^\circ\text{C}$. The solid was collected, washed with pentane (3 x 5 mL) and dried under vacuum to give **2.40b** (83 mg, 0.126 mmol) as a blue-green solid. Yield: 85%. ^1H NMR (CD_2Cl_2): δ 17.35 (s,

1 H, Ru=CH), 7.62 (d, $J = 7.8$ Hz, 1 H, Aryl H), 7.49 (t, $J = 7.8$ Hz, 1 H, Aryl H), 7.18 (t, $J = 6.9$ Hz, 1 H, Aryl H), 7.14 (s, 1 H, Mes), 7.03 (s, 1 H, Mes), 6.88 (s, 1 H, Mes), 6.81 (d, $J = 7.5$ Hz, 1 H, Aryl H), 5.94 (s, 1 H, Mes), 4.18–3.71 (m, 4 H, $\text{NCH}_2\text{CH}_2\text{N}$), 2.72 (s, 3 H, Mes- CH_3), 2.61 (s, 3 H,

Mes-CH₃), 2.48 (s, 3 H, Mes-CH₃), 2.36 (s, 3 H, Mes-CH₃), 2.16 (s, 3 H, Mes-CH₃), 1.51 (s, 3 H, Mes-CH₃), 1.29 (s, 3 H, SCMe₃). ¹³C{¹H} NMR (CD₂Cl₂): δ 287.54 (Ru=CH), 213.74 (Ru-C(N)₂), 156.58, 140.46, 140.25, 138.58, 138.18, 137.59, 136.05, 135.68, 132.69, 130.91, 130.57, 130.46, 129.80, 129.72, 129.61, 129.01, 124.20, 54.48, 51.91, 51.62, 30.68, 21.39, 21.18, 20.63, 20.22, 19.18, 18.00. HRMS-FAB (m/z): [M]⁺ calcd for C₃₂H₄₀Cl₂N₂SRu, 656.1333; found, 656.1307.

RCM of 2.18 at 25 °C. 1 mol% catalyst was added to a 0.1 M solution of **2.18** in CH₂Cl₂. The reaction was allowed to proceed at 25 °C and was monitored by gas chromatography.

RCM of 2.18 at variable temperature. In the dry box, 2.5 mol% catalyst (0.0052 mmol) was dissolved in C₆D₆ (0.65 mL) in an NMR tube fitted with a teflon septum screw-cap. The resulting solution was allowed to equilibrate in the NMR probe at 40 °C. **2.18** (50 μL, 0.207 mmol, 0.30 M) was injected into the NMR tube neat and the reaction was monitored by ¹H NMR spectroscopy. The olefinic resonances integrals of the product relative to that of the starting material were measured with the residual protio solvent peak used as an internal standard.

RCM of 2.18 under standard conditions. A stock solution was prepared to deliver the catalyst solution. Inside a glovebox, a volumetric flask was charged with catalyst (0.016 mmol) and CD₂Cl₂ added to prepare 1.0 mL of stock solution (0.016 M). An NMR tube with a screwcap septum top was charged with catalyst stock solution (0.016 M, 50 μL, 0.80 μmol, 1.0 mol%) and CD₂Cl₂ (0.75 mL). The sample was equilibrated at 30 °C in the NMR probe before **2.18** (19.3 μL, 19.2 mg, 0.080 mmol, 0.1 M) was added via syringe. Data points were collected over an appropriate period of time using the Varian array function. The conversion to **2.19** was determined by comparing the ratio of the integrals of the methylene protons in the starting material, δ 2.61 (dt), with those in the product, δ 2.98 (s).

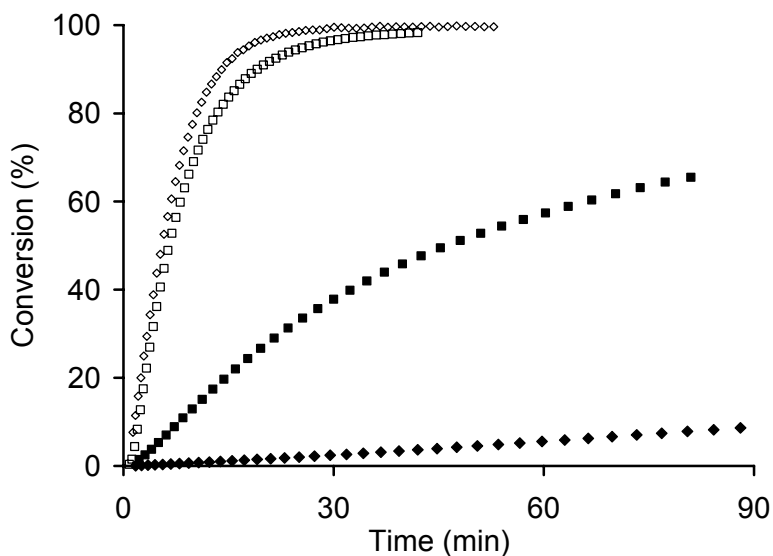


Figure 2.21. Conversion plot for RCM of **2.18** with **2.1** (\diamond), **2.2** (\square), and **2.31a** (\blacksquare), and **2.31e** (\blacklozenge) (1.0 mol%, 30 °C, 0.1 M CD_2Cl_2).

ROMP of DCPD. Dicyclopentadiene containing 3.5% tricyclopentadiene (100 g) was polymerized by addition of catalyst (monomer/catalyst = 30,000) at 30 °C. The reaction was monitored by measuring the polymerization exotherm.

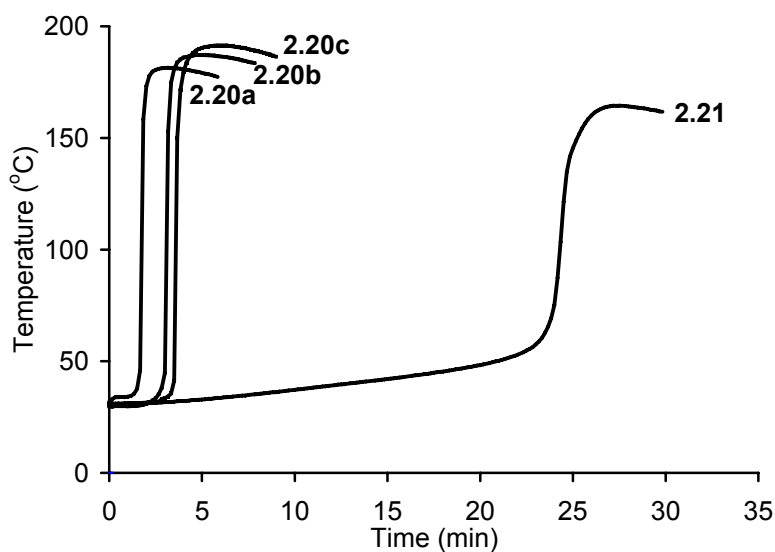


Figure 2.22. Exotherm plot for ROMP of DCPD with **2.20a–c**, **2.21** (30,000:1 M/C, 30 °C).

Test of sulfur inhibition in 2.33c. A stock solution was prepared to deliver the catalyst solution. Inside a glovebox, a volumetric flask was charged with catalyst **2.33a** (0.026 mmol) and C_6D_6 added to prepare 2.0 mL of catalyst stock solution (0.013 M). A stock solution of SMe_2 was

prepared by dissolving SMe_2 (30.3 μL , 25.6 mg, 0.41 mmol) and C_6D_6 added to prepare 2.0 mL of solution (0.21 M). An NMR tube with a screwcap septum top was charged with catalyst stock solution (0.013 M, 0.40 mL, 5.2 μmol , 2.5 mol%), SMe_2 stock solution (25 μL , 5.2 μmol) and C_6D_6 (0.25 mL). The sample was equilibrated at 60 $^\circ\text{C}$ in the NMR probe before **2.18** (50 μL , 50 mg, 0.21 mmol, 0.3 M) was added via syringe. Data points were collected over an appropriate period of time using the Varian array function. The conversion to **2.19** was determined by comparing the ratio of the integrals of the methylene protons in the starting material, δ 2.84 (dt), with those in the product, δ 3.14 (s). Corresponding NMR samples were prepared with **2.33a** and **2.33c** in the absence of SMe_2 .

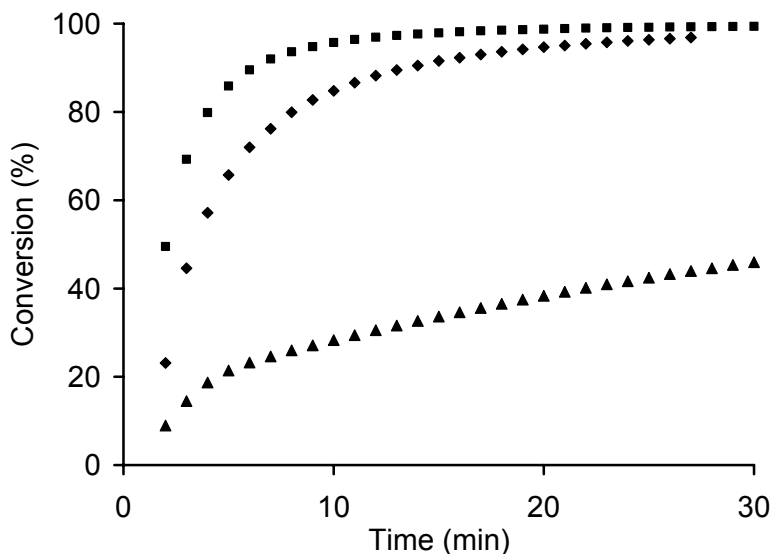


Figure 2.23. Conversion plot for RCM of **2.18** with **2.33a** (■), **2.33a** + 1 eq SMe_2 (◆), and **2.33c** (▲) (2.5 mol%, 65 $^\circ\text{C}$, 0.3 M C_6D_6).

X-ray crystallographic data. Crystallographic data for the structures in this chapter have been deposited at the CCDC, 12 Union Road, Cambridge, CB2 1EZ, UK and copies can be obtained on request, free of charge, via <http://www.ccdc.cam.ac.uk/conts/retrieving.html>.

Table 2.3. X-ray Crystallographic Data

Complex	2.20a (CCDC 259695)	2.21 (CCDC 259696)	2.25a (CCDC 278062)
Empirical Formula	C ₂₉ H ₃₅ Cl ₂ N ₃ Ru	C ₂₉ H ₃₅ Cl ₂ N ₃ Ru · CH ₂ Cl ₂	C ₃₄ H ₄₃ Cl ₂ N ₃ Ru
Formula Weight	597.57	682.50	665.68
λ (Å)	0.71073	0.7103	0.7103
T (K)	100(2)	100(2)	100(2)
<i>a</i> (Å)	8.5295(2)	8.7869(4)	13.7555(7)
<i>b</i> (Å)	11.8164(2)	14.1539(7)	11.4276(6)
<i>c</i> (Å)	13.9583(3)	23.9944(12)	20.4538(11)
α (°)	84.9350(10)		
β (°)	81.3450(10)	93.7840(10)	98.6480(10)
γ (°)	80.0880(10)		
<i>V</i> (Å ³)	1367.23(5)	2977.7(2)	3178.6(3)
<i>Z</i>	2	4	4
Crystal System	Triclinic	Monoclinic	Monoclinic
Space Group	P-1	P2 ₁ /c	P2 ₁ /n
d_{calc} (g/cm ³)	1.452	1.522	1.391
θ range (°)	1.75 to 45.08	1.67 to 28.38	1.67 to 27.55
μ (mm ⁻¹)	0.791	0.911	0.689
GOF on F ²	1.263	1.749	2.222
<i>R</i> ₁ , <i>wR</i> ₂ [<i>I</i> > 2 σ (<i>I</i>)]	0.0382, 0.0751	0.0347, 0.0595	0.0593, 0.1034

Complex	2.31a (CCDC 254980)	2.31e (CCDC 272587)	2.33c (CCDC 281471)
Empirical Formula	C ₃₃ H ₄₁ Cl ₂ N ₃ Ru	C ₂₈ H ₃₉ Cl ₂ N ₃ Ru	C ₃₀ H ₄₃ Cl ₂ N ₃ RuS · ½(C ₄ H ₈ O)
Formula Weight	651.66	589.59	685.76
λ (Å)	0.71073	0.71073	0.71073
T (K)	100(2)	100(2)	100(2)
a (Å)	13.5715(4)	14.9244(9)	11.1365(3)
b (Å)	11.6530(4)	16.4672(10)	17.4341(4)
c (Å)	20.2953(6)	11.2788(7)	34.7895(9)
α (°)			
β (°)	100.8070(10)		93.7070(1)
γ (°)			
V (Å ³)	3152.75(17)	2771.9(3)	6740.4(3)
Z	4	4	8
Crystal System	Monoclinic	Orthorhombic	Monoclinic
Space Group	P2 ₁ /c	Pnmm	Pc
d _{calc} (g/cm ³)	1.373	1.413	1.352
θ range (°)	1.67 to 47.34	1.84 to 33.52	1.17 to 38.31
μ (mm ⁻¹)	0.693	0.779	0.712
GOF on F ²	1.358	1.576	1.302
R ₁ , wR ₂ [I > 2σ(I)]	0.0514, 0.0848	0.0575, 0.0784	0.0580, 0.0946

Complex	2.37a (CCDC 272875)	2.39b (CCDC 633023)	2.40b (CCDC 633024)
Empirical Formula	C ₃₃ H ₄₃ Cl ₂ N ₃ Ru	C ₃₇ H ₄₅ Cl ₂ N ₃ SRu & C ₃₂ H ₄₀ Cl ₂ N ₂ SRu	C ₃₂ H ₄₀ Cl ₂ N ₂ SRu · C ₆ H ₆
Formula Weight	653.67	1392.48	734.80
λ (Å)	0.71073	0.71073	0.71073
T (K)	100(2)	100(2)	100(2)
<i>a</i> (Å)	11.2474(5)	34.7735(11)	17.963(3)
<i>b</i> (Å)	10.3295(4)	14.7770(5)	16.328(2)
<i>c</i> (Å)	27.6856(12)	12.7559(4)	24.783(4)
α (°)			
β (°)	100.7010(10)		100.438(3)
γ (°)			
<i>V</i> (Å ³)	3160.6(2)	6554.6(4)	7148.3(18)
Z	4	4	8
Crystal System	Monoclinic	Orthorhombic	Monoclinic
Space Group	P2 ₁ /n	Pca2 ₁	P2 ₁ /n
d_{calc} (g/cm ³)	1.374	1.411	1.366
θ range (°)	1.86 to 38.36	1.50 to 34.06	1.54 to 25.09
μ (mm ⁻¹)	0.691	0.732	0.675
GOF on F ²	1.194	1.301	2.492
R_{11} , wR_{22} [$I > 2\sigma(I)$]	0.0575, 0.0807	0.0470, 0.0689	0.0895, 0.1628

References and Notes

- ¹ Grubbs, R. H., Ed. *Handbook of Metathesis*; Wiley-VCH: Weinheim, Germany, 2003.
- ² Trnka, T. M.; Grubbs, R. H. *Acc. Chem. Res.* **2001**, *34*, 18–29.
- ³ Scholl, M.; Ding, S.; Lee, C. W.; Grubbs, R. H. *Org. Lett.* **1999**, *1*, 953–956.
- ⁴ (a) Garber, S. B.; Kingsbury, J. S.; Gray, B. L.; Hoveyda, A. H. *J. Am. Chem. Soc.* **2000**, *122*, 8168–8179. (b) Gessler, S.; Randl, S.; Blechert, S. *Tetrahedron Lett.* **2000**, *41*, 9973–9976.
- ⁵ (a) Sanford, M. S.; Ulman, M.; Grubbs, R. H. *J. Am. Chem. Soc.* **2001**, *123*, 749–750. (b) Sanford, M. S.; Love, J. A.; Grubbs, R. H. *J. Am. Chem. Soc.* **2001**, *123*, 6543–6554.
- ⁶ Dias, E. L.; Nguyen, S. T.; Grubbs, R. H. *J. Am. Chem. Soc.* **1997**, *119*, 3887–3897.
- ⁷ Louie, J.; Grubbs, R. H. *Organometallics* **2002**, *21*, 2153–2164.
- ⁸ van der Schaaf, P. A.; Kolly, R.; Kirner, H.-J.; Rime, F.; Mühlebach, A.; Hafner, A. *J. Organomet. Chem.* **2000**, *606*, 65–74.
- ⁹ For an example see: Hejl, A.; Scherman, O. A.; Grubbs, R. H. *Macromolecules* **2005**, *38*, 7214–7218.
- ¹⁰ Chang, S.; Jones, L. II.; Wang, C.; Henling, L. M.; Grubbs, R. H. *Organometallics* **1998**, *17*, 3460–3465.
- ¹¹ Allaert, B.; Dieltiens, N.; Ledoux, N.; Vercaemst, C.; Van Der Voort, P.; Stevens, C. V.; Linden, A.; Verpoort, F. *J. Mol. Catal. A: Chem.* **2006**, *260*, 221–226.
- ¹² Denk, K.; Fridgen, J.; Herrmann, W. A. *Adv. Synth. Catal.* **2002**, *344*, 666–670.
- ¹³ Sanford, M. S.; Henling, L. M.; Day, M. W.; Grubbs, R. H. *Angew. Chem. Int. Ed.* **2000**, *39*, 3451–3453.
- ¹⁴ Michrowska, A.; Bujok, R.; Harutyunyan, S.; Sashuk, V.; Dolgonos, G.; Grela, K. *J. Am. Chem. Soc.* **2004**, *126*, 9318–9325.
- ¹⁵ Gulajski, L.; Michrowska, A.; Bujok, R.; Grela, K. *J. Mol. Catal. A: Chem.* **2006**, *254*, 118–123.
- ¹⁶ Fürstner, A.; Thiel, O. R.; Lehmann, C. W. *Organometallics* **2002**, *21*, 331–335.
- ¹⁷ Slugovc, C.; Perner, B.; Stelzer, F.; Mereiter, K. *Organometallics* **2004**, *23*, 3622–3626.
- ¹⁸ Bennett, M. A.; Nyholm, R. S.; Saxby, J. D. *J. Organomet. Chem.* **1967**, *10*, 301–306.
- ¹⁹ Sanford, M. S.; Love, J. A.; Grubbs, R. H. *Organometallics* **2001**, *20*, 5314–5318.
- ²⁰ Chatterjee, A. K.; Choi, T.-L.; Sanders, D. P.; Grubbs, R. H. *J. Am. Chem. Soc.* **2003**, *125*, 11360–11370.
- ²¹ Benitez, D.; Goddard, W. A., III *J. Am. Chem. Soc.* **2005**, *127*, 12218–12219.
- ²² (a) A related complex with cis neutral ligands and cis anionic pentafluorophenoxide ligands has been reported: Conrad, J. C.; Amoroso, D.; Czechura, P.; Yap, G. P. A.; Fogg, D. E. *Organometallics* **2003**, *22*, 3634–3636. (b) A related vinylcarbene ruthenium complex containing

cis chlorides has also been reported: Trnka, T. M.; Day, M. W.; Grubbs, R. H. *Organometallics* **2001**, *20*, 3845–3847.

²³ Barbasiewicz, M.; Szadkowska, A.; Bujok, R.; Grela, K. *Organometallics* **2006**, *25*, 3608–3613.

²⁴ Ung, T.; Hejl, A.; Grubbs, R. H.; Schrodi, Y. *Organometallics* **2004**, *23*, 5399–5401.

²⁵ Wakamatsu, H.; Blechert, S. *Angew. Chem. Int. Ed.* **2002**, *41*, 2403–2405.

²⁶ Grela, K.; Harutyunyan, S.; Michrowska, A. *Angew. Chem. Int. Ed.* **2002**, *41*, 4038–4040.

²⁷ Slugovc, C.; Burtscher, D.; Stelzer, F.; Mereiter, K. *Organometallics* **2005**, *24*, 2255–2258.

²⁸ Allinger, N. L.; Zalkow, V. J. *J. Org. Chem.* **1960**, *25*, 701–704.

²⁹ Zhang, J.; Gunnoe, T. B. *Organometallics* **2003**, *22*, 2291–2297.

³⁰ Sanford, M.S. Ph.D. Thesis, California Institute of Technology, 2001.

³¹ Ritter, T.; Hejl, A.; Wenzel, A. G.; Funk, T. W.; Grubbs, R. H. *Organometallics* **2006**, *25*, 5740–5745.

³² For **17c**, four unique but similar molecules crystallize in the unit cell. The distances and angles for one molecule have been reported in the text.

³³ Hejl, A.; Day, M. W.; Grubbs, R. H. *Organometallics* **2006**, *25*, 6149–6154.

³⁴ Cotton, F. A.; Wilkinson, G.; Murillo, C. A.; Bochmann, M. *Advanced Inorganic Chemistry*, 6th Ed; Wiley-Interscience: New York, 1999.

³⁵ Peters, R. G.; Warner, B. P.; Scott, B. L.; Burns, C. J. *Organometallics* **1999**, *18*, 2587–2589.

³⁶ Pangborn, A. B.; Giardello, M. A.; Grubbs, R. H.; Rosen, R. K.; Timmers, F. J. *Organometallics* **1996**, *15*, 1518–1520.

³⁷ Katayama, H. *Chem. Pharm. Bull.* **1978**, *26*, 2027–2035.

³⁸ Cocker, W.; Geraghty, N. W. A.; McMurry, T. B. H.; Shannon, P. V. R. *J. Chem. Soc., Perkin Trans. 1* **1984**, 2245–2254.

³⁹ Noack, M.; Göttlich, R. *Eur. J. Inorg. Chem.* **2002**, 3171–3178.

⁴⁰ Bender, C. F.; Widenhoefer, R. A. *J. Am. Chem. Soc.* **2005**, *127*, 1070–1071.

⁴¹ Clark, P. W.; Curtis, J. L. S.; Garrou, P. E.; Hartwell, G. E. *Can. J. Chem.* **1974**, *52*, 1714–1720.